

# Biological Random Walks: multi-omics integration for disease gene prioritization

Michele Gentili<sup>1</sup>, Leonardo Martini<sup>1</sup>, Marialuisa Sponziello<sup>2</sup>, and Luca Becchetti<sup>1</sup>

<sup>1</sup>Department of Computer, Control, and Management Engineering Antonio Ruberti, Sapienza University of Rome, Rome, Italy

<sup>2</sup>Translational and Precision Medicine Department Sapienza University of Rome, Rome, Italy

## Abstract

**Motivation:** Over the past decade, network-based approaches have proven useful in identifying disease modules within the human interactome, often providing insights into key mechanisms and guiding the quest for therapeutic targets. This is all the more important, since experimental investigation of potential gene candidates is an expensive task, thus not always a feasible option. On the other hand, many sources of biological information exist beyond the interactome and an important research direction is the design of effective techniques for their integration.

**Results:** In this work, we introduce the Biological Random Walks (BRW) approach for disease gene prioritization in the human interactome. The proposed framework leverages multiple biological sources within an integrated framework. We perform an extensive, comparative study of BRW’s performance against well-established baselines.

**Availability and implementation:** All code is publicly available and can be downloaded at <https://github.com/LeoM93/BiologicalRandomWalks>. We used publicly available datasets, details on their retrieval and preprocessing are provided in the supplementary material.

**Supplementary material:** Supplementary material available.

## 1 Introduction

In recent years, through the advent of big data, genomics, and quantitative *in silico* methodologies, medicine is witnessing tremendous advancements towards the understanding of the human pathophysiology. [SSA<sup>+</sup>20]. Gene-disease associations have been identified by genome-wide association studies (GWAS) [HS09] and more recently by whole exome or whole genome sequencing studies [KSL<sup>+</sup>13]. While many of the mechanisms underlying these associations remain largely unclear, a growing body of research highlights associations between groups of interacting proteins and diseases within the so-called “human interactome”, representing the cellular network of all physical molecular interactions [BGL11]. A key feature is that disease proteins do not appear to be uniformly scattered across the interactome [MSK<sup>+</sup>15], but they are prone to participation in common biological activities such as, for example, genome maintenance, cell differentiation or growth signaling, which are the most relevant pathways in carcinogenesis [ODC<sup>+</sup>18]. For these reasons, while traditional single protein (i.e., magic bullet) approaches have limited effectiveness in addressing complex diseases, network-based ones can prove useful in identifying disease modules within the interactome, hopefully providing insights into key mechanisms and guiding the quest for therapeutic targets. Moreover, experimental investigation of potential gene candidates is an expensive task, thus not always a feasible option.

The human interactome refers to all protein-protein interactions within a cell, including regulatory interaction of transcription factors, metabolic enzyme-coupled interactions, protein complexes, and kinase/substrate interactions. This network is largely incomplete. Currently, more than 140,000 interactions involving over 13,000 proteins are known (e.g., see [KSSF17, GNZ<sup>+</sup>14]). The interactome-based approach to network medicine [BGL11] proved effective for a number of diseases, e.g., by identifying putative biomarkers and subtypes, thus allowing a principled approach to drug targeting [BGL11, ODC<sup>+</sup>18]. The need for new disease genes (or disease proteins) as putative candidates for

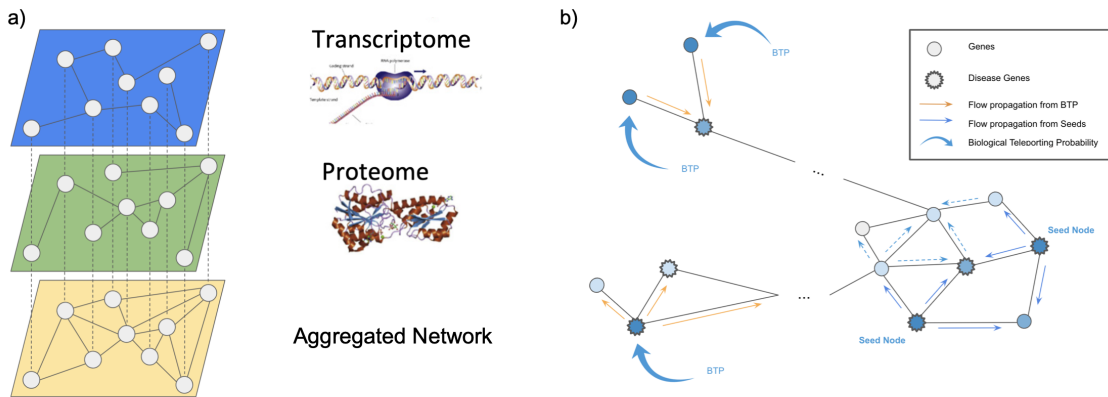


Figure 1: Network aggregation and network flow of Biological Random Walks. a) shows the pre-processing step that combines PPI and CO-Expression topology to derive a combined network. The transition matrix of PPI and CO-Expression network are combined using a convex combination to compute an aggregated transition matrix. Note that what is termed “aggregated network” in tab a) is actually a *weighted* network that corresponds to the aggregated transition matrix. b) Shows the flow of the random walker when the personalization vector is biased with disease specific information. In this way the flow can propagate from seed nodes (i.e., known disease genes), but also from node that are not part of the seed set but biologically similar to it (i.e., biological teleporting probability (BTP)).

diagnosis, prognosis or treatment, motivated the development of a number of algorithms for disease genes and modules prediction [GMB15].

Two related classes of methodologies have emerged over the last decade as the most promising: module-based [GMB15, BGL11] and network propagation [CIRS17, KBHR08] algorithms. Module-based algorithms find topological, functional or disease modules in the interactome network, on the hypothesis that these represent cellular components likely involved in the same disease. Network propagation (or diffusion-based) algorithms leverage the information flow through nearby proteins in the network from initial (known) disease genes as their main ingredient.

While important and effective in many cases, the interactome is only one of many sources of biological information. An important research direction is the quest for effective techniques that allow the seamless integration of rich and heterogeneous biological sources into methods that were originally designed to leverage the topological features of the interactome [DHH<sup>+</sup>18, SL20, DBTVOM07].

**Our contribution** In this work, we introduce the Biological Random Walks (BRW) framework for disease gene prioritization. The proposed framework leverages the integration of multiple biological sources within a propagation-based approach. We compare BRW’s performance against well-established baselines, such as: RWR [NK10], DIAMOnD [GMB15], DADA [EBEK11] and RWR-M [VTN<sup>+</sup>19]. In particular, we investigate BRW’s performance along different axes: i) an in-depth, comparative analysis on four cancer phenotypes (i.e., breast cancer, lung adenocarcinoma, papillary thyroid cancer, colorectal adenocarcinoma); ii) a broad comparative analysis of BRW’s prioritization performance over a wide spectrum of Mendelian diseases with different characteristics and prior information available; iii) an external validation using FDA approved drugs for Breast Cancer treatment, along with an evaluation of the algorithm results’ stability across multiple population studies. <sup>1</sup>.

## 2 Materials and Methods

### 2.1 Biological Random Walks

Biological Random Walks (BRW) build on the hypothesis that integrating different biological information sources may better reflect the complexity of protein interactions in a cell’s process. In light of this insight, our approach integrates information on pairwise protein interaction of the Protein-Protein Interaction network (PPI) [BGL11] with other biological data in a unified framework. Our approach is to some extent agnostic to the particular biological data source, as long as it affords a principled notion of similarity between proteins. In the remainder, we use bold lowercase to denote vectors and capital, non-bold letters to denote matrices. Given a vector  $\mathbf{x}$ ,  $x_i$  denotes its  $i$ -th entry.

**Notation.** We represent the PPI as an undirected graph  $G = (V, E)$ , with genes as vertices. Any edge  $(i, j)$  represents a known protein-protein interaction recorded in the PPI. We assume  $|V| = n$  in the following. For a given gene  $i$ ,  $N_h(i)$  denotes the subset of  $G$ ’s vertices whose shortest path distance from  $i$  is exactly  $h$ .

#### 2.1.1 Random Walks with Restart

Random Walk with Restart (RWR) [KBHR08] is a diffusion-based method, whose purpose is identifying disease modules that are topologically “close” to known disease genes in the interactome. It was shown to outperform other prioritization algorithms in many cases [NK10]. In a nutshell, this algorithm can be seen as performing multiple random walks over the PPI network, each starting from a *seed node* associated to a known disease gene, iteratively moving from one node to a random neighbour, thus simulating the diffusion of the disease phenotype across the interactome. More formally, the random walk with restart is defined as:

$$\mathbf{p}^{(t+1)} = (1 - r)W\mathbf{p}^{(t)} + r\mathbf{q}. \quad (1)$$

Here,  $W$  is the column-normalized adjacency matrix of the graph and  $\mathbf{p}^{(t)}$  is a vector, whose  $i$ -th entry  $p_i^{(t)}$  is the probability of the random walk being at node  $i$  at the end of the  $t$ -th step.  $r \in (0, 1)$  is the restart probability, i.e., the probability that the random walk is restarted from one of the (disease-associated) seed nodes in the next step. Upon a restart, the probability of restarting the random walk from some seed node  $j$  is  $q_j$ . Vector  $\mathbf{q}$  is normally called a *personalization vector* in the Data Science literature. This random walk corresponds to an ergodic Markov chain [LP17] that admits a stationary distribution (i.e., a fixed point)  $\mathbf{p}$ . Nodes of the PPI are simply ranked by considering the corresponding entries of  $\mathbf{p}$  in descending order of magnitude.

#### 2.1.2 Biological Information-Aware Random Walks

For the sake of exposition, in the remainder we refer to the biological information associated to a gene (e.g., the set of its annotations) as the set of its *features*. These can include (more precisely, be derived from) annotations from the Gene Ontology database [Con19] (GO in the remainder) or gene expression levels. We remark that, in principle, any reliable information source on gene biology can be integrated. BRW ranks genes according to the main steps outlined below.

Unlike [KBHR08] and similar approaches, our method consists of two main steps: i) extracting statistically significant features from biological data, using them to compute a personalization vector and a transition matrix used by the BRW algorithm; ii) using the stationary distribution of the corresponding random walk to rank genes. Our approach to computing aggregated personalization vectors and transition matrices is outlined below, with further details given in Sections B.3 and B.4 of the supplementary material.

---

<sup>1</sup>Some of the ideas presented in this submission, albeit in preliminary form and accompanied by a minimal, internal validation, appeared in [GMP+19]. For the sake of completeness, Supplementary Section C.4 presents a comparison of our approach with [GMP+19]

**Computing a Personalization Vector.** Both gene annotation data and gene expression levels allow derivation of personalization vectors that reflect some notion of similarity between a gene and a disease, with the latter represented by the set of its seed genes. In the first case, this similarity is defined in terms of knowledge about genes’ involvement in various biological functions and/or diseases. In the second case, similarity is defined in terms of co-expression levels of different genes in subject cases as opposed to expression levels in a control group, using data about a population of patients involved in a clinical trial.

For annotation data, assume we have  $\ell$  sources of biological information (e.g., GO, KEGG pathways etc.). Let  $S$  denote the seed set. For every  $j = 1, \dots, \ell$ , we use  $\mathcal{F}^j$  to denote the subset of annotations from the  $j$ -th source that are associated with at least one gene in  $S$ . Then, for every  $j = 1, \dots, \ell$ , we select a subset of annotations  $\widehat{\mathcal{F}}^j$ , filtering out annotations that are not statistically significant, as shown in Supplementary Figure 2 (i.e.,  $p$ -value  $> 10^{-5}$ , using Fisher Exact Test and FDR correction), so that  $\mathcal{F} = \cup_{j=1}^{\ell} \widehat{\mathcal{F}}^j$  denotes the set of all statistically significant annotations that are associated with genes in  $S$ . Likewise, for every gene  $i$  (not necessarily belonging to  $S$ ), we denote by  $\mathcal{A}(i)$  the set of its annotations, possibly extracted from multiple biological information sources. We assign each gene  $i$  a weight  $\theta_i$ , which reflects the extent to which  $i$  shares annotations that are statistically significant for genes that belong to the seed set of the disease under consideration. While other choices are possible, the definition we adopted reflects the extent of the *inclusion* of  $\mathcal{A}_i$  in each of the  $\ell$  sources:

$$\theta_i = \sum_{j=1}^{\ell} \frac{|\mathcal{A}(i) \cap \widehat{\mathcal{F}}^j|}{|\widehat{\mathcal{F}}^j|}. \quad (2)$$

At this point, the components of a personalization vector  $\mathbf{q}$  can be computed as follows:

$$q_i = \frac{\theta_i}{\sum_{i=0}^N \theta_i}, \quad (3)$$

with  $N$  the number of genes we consider. Note that  $q_i$  denotes the probability that, upon teleportation, the random walkers jumps to gene  $i$ . Further details are given in Section B.3.1 of the Supplementary material.

We next discuss how to compute personalization vectors from gene expression data. An important goal is the identification of Differentially Expressed (DE) genes, whose expression levels systematically differ between case (Breast Cancer Cells) and a control group (Normal Breast Cells). We follow the approach proposed in [MGS<sup>+</sup>17], in which subjects of the control group are assigned personalized perturbation profiles (PEEPs), from which gene expression-aware personalization vectors can be derived. Succinctly put, for each gene  $i$  and for each subject  $j$ , the expression level  $l_i^j$  of gene  $i$  in subject  $j$  is compared with the distribution of the expression level of gene  $i$  within the control group by taking the corresponding z-score  $z_{ij}$ . This approach allows association of a “bar code” to each subject. Following [MGS<sup>+</sup>17], we set  $|z_{ij}| > 2.5$  as the threshold to declare gene  $i$  differentially expressed in subject  $j$ . Following the general intuition stated in the introduction that disease genes generally are not scattered across the interactome, we also bias our choice towards differentially expressed genes that are closer to disease genes in the PPI. Eventually, we obtain a personalization vector  $\mathbf{q}$  that reflects both genes’ differential expressions and vicinity to disease genes. For full details on computing PEEP and deriving gene expression-aware personalization vectors, we refer the reader to Supplementary Section B.3.1.

**Computing a Transition Matrix.** Similar approaches can be used to derive a transition matrix for the random walk with restart. Both approaches rely on the PPI, differing on the way PPI’s edges are assigned weights that reflect genes’ similarity and determine the probabilities of edge traversals. We leverage categorical, biological information (e.g., gene annotations) by defining a weighted transition matrix  $W$ , in which each entry  $W_{ij}$  depends on the extent to which nodes/genes  $i$  and  $j$  of the PPI share common annotations (i.e., they are involved in common biological processes) that are also significant for the disease. In more detail, considered genes  $i$  and  $j$ , we define the following *Disease Specific Interaction Function* (DSI function in the remainder):

$$DSI(i, j) = |\mathcal{A}(i) \cap \mathcal{A}(j) \cap \mathcal{F}|, \quad (4)$$

<sup>2</sup>It should be noted that [KBHR08] corresponds to choosing  $\theta_i = 1$  if  $i \in S$ ,  $\theta_i = 0$  otherwise.

where we remind that  $\mathcal{A}(k)$  denotes the set of gene  $k$ 's annotations, while  $\mathcal{F}$  denotes the overall set of annotations that are statistically significant for disease genes. Intuitively, the higher  $DSI(i, j)$ , the more  $i$  and  $j$  share annotations that are also statistically significant for the disease under consideration. In the end, edges in the PPI will be assigned weights depending on the DIS function as follows:

$$W_{ij} = \begin{cases} c + DSI(i, j) & \text{if } (i, j) \in E, \\ 0 & \text{otherwise.} \end{cases} \quad (5)$$

Here,  $c$  is a positive constant that accounts for usual sparsity of the available datasets, so that no biological information may be available for the end-points of a link in the PPI. In this case, the link receives a minimum weight  $c$ . As with personalization vectors, gene expression information about a population of patients can also be used to define a tissue-specific, population-dependent transition matrix. Specifically, gene expression information is used to assign weights to edges of the underlying PPI network, this time reflecting similarities between genes in terms of co-expression with respect to the subject population. Consider a CO-Expression network in which each pair of genes  $(i, j)$  is assigned a score equal to the Pearson's correlation coefficient  $pc_{i,j}$  between the expression levels of  $i$  and  $j$  within the population. We can define a transition matrix  $W$  by assigning each edge  $(i, j)$  of the PPI network a probability as follows:

$$W_{ij} = \frac{|pc_{ij}|}{\sum_{k \in N(i)} |pc_{ik}|} \quad (6)$$

where  $N(i)$  is the set of  $i$ 's neighbors in the PPI network. Note that i) for every node/gene  $i$  we consistently have a probability distribution over its incident edges and ii) the importance of edges reflects the absolute value of the correlation between the expression levels of two genes within the population of interest.

**Integrating Biological Information and Gene Expression.** We discussed above two orthogonal approaches to the design of personalization vectors. The first one leverages similarities between the biological processes associated to known disease proteins and those to be prioritized. Hence, teleporting probabilities depend on the seed set through association with common biological processes. In the second case, teleporting probabilities depend on information that is tissue-specific (the level of expression in a population of subjects affected by a certain disease) and partly on the seed set, but this time through the PPI's topology. Hence, these two approaches largely rely on complementary sources of information. In order to integrate these complementary sources into a unique personalization vector that leverages both, we follow a simple, yet mathematically principled approach, whereby we take a *convex combination* of the corresponding personalization vectors. Namely, assume we have computed two personalization vectors  $\mathbf{q}_1$  and  $\mathbf{q}_2$ , the former using biological information only, the latter using gene expression data and the PPI. We obtain a personalization vector as follows:

$$\mathbf{q} = \alpha \mathbf{q}_1 + (1 - \alpha) \mathbf{q}_2, \quad (7)$$

where  $\alpha \in [0, 1]$ . Parameter  $\alpha$  allows to weigh in the relative importance of the different information sources we are using. Intuitively, this type of aggregation amounts to considering a gene a potential candidate if it is statistically significant in terms of its involvement in biological processes, of its gene expression levels in the subject group, or both.<sup>3</sup> The choice of  $\alpha$  (and other parameters of the model), its impact on performance and dependence of the optimal choice on the scenario at hand are discussed in detail in Sections 3, 4 and in Section C.2 of the supplementary material. **Remark.** Despite its simplicity, this is a mathematically principled choice. In particular, it is well-known [JW03] and easy to show that the stationary distribution corresponding to the convex combination of two personalization vectors  $\mathbf{q}_1$  and  $\mathbf{q}_2$  is itself the linear combination of the stationary distributions corresponding to  $\mathbf{q}_1$  and  $\mathbf{q}_2$  respectively. Briefly put, the parameter  $\alpha$  allows us to tune the relative importance of the information provided by gene annotations and gene expression levels respectively. Moreover, this approach extends seamlessly to an arbitrary number of heterogeneous sources of information (and corresponding personalization vectors). Other aggregation methods were also considered, yet they provided worse or at most comparable results. Some are presented in Section B.3.2 of the

<sup>3</sup>Note that this approach seamlessly extends to an arbitrary number of information sources.

Supplementary material for the sake of completeness. In the previous paragraphs, we have seen how we can derive random walk transition matrices using only information about biological processes (i.e., annotations) or gene expression data from a population of subjects. As with personalization vectors, multiple transition matrices derived from complementary biological sources can be integrated into a single *aggregate transition matrix*. For example, assume we computed transition matrices  $W_1$  and  $W_2$  using biological and gene expression information respectively. Any convex combination of  $W_1$  and  $W_2$  is a feasible transition matrix. Namely, for some  $\beta \in [0, 1]$ , we consider the transition matrix

$$W = \beta W_1 + (1 - \beta) W_2.$$

It is easy to see that i)  $W$  is still a transition matrix, i.e., the entries of each row sum to one and that ii) the approach seamlessly extends to any number of complementary sources. In the case of biological annotations and gene expression data,  $\beta = 1$  corresponds to only considering biological annotations, whereas  $\beta = 0$  corresponds to only leveraging gene expression data. So,  $\beta$  is a parameter, whose tuning allows us to weigh the importance of one source of information with respect to the other.

## 3 Results

This section investigates BRW’s performance in prioritizing gene candidates for genetic diseases.

### 3.1 Experimental Setup

We used a number of biological data sources. Some of them were used as inputs, to define key parameters of our algorithms, while others were used to biologically validate the results of the algorithms we considered. They are briefly described here and more extensively in Section A of the supplementary material.

**Data sources.** The experiments discussed in Section 3 were conducted on the HIPPIE Protein-Protein Interaction network (PPI) [ALANS16] and on the same Protein-Protein Interaction network (PPI) as in [GMB15] for the sake of comparison.

We used three different sources of gene biological information: Gene Ontology Consortium<sup>4</sup> where, for each gene, we downloaded its biological processes, KEGG [Kan19, KSF<sup>+</sup>18, KG00] and Reactome [JMV<sup>+</sup>19], which we used to download pathways’ annotations. Gene expression datasets were downloaded from The Cancer Genome Atlas database<sup>5</sup>.

We validated the methods considered in this study both via an internal validation on known disease genes and through an external validation using drug target associations. In more detail, we used disease-gene associations as in [GMB15] that describe a corpus of 70 Mendelian diseases. From [PRASP<sup>+</sup>20], we further derived known disease-gene associations for the four different cancer types that we investigate in Section 3 (i.e, breast cancer, lung adenocarcinoma, papillary thyroid cancer, colorectal adenocarcinoma). Finally, we used Drug-Gene Target associations from DrugBank<sup>6</sup> [WDG<sup>+</sup>17]. We selected only drugs approved for Breast Cancer treatment from Food and Drug Administration<sup>7</sup> (Supplementary Table 2).

All data sources mentioned above are more extensively discussed in Section A of the supplementary material.

**Baselines.** To provide a robust performance assessment, we compared BRW with a number of well-known, state-of-art baselines for disease gene prioritization, namely, RWR [KBHR08], DIAMOnD [GMB15], DADA [EBEK11] and RWR-M [VTN<sup>+</sup>19]. For the sake of completeness, supplementary Section C.4 also compares our approach against an embryonic (and underperforming) version of our framework that was presented in [GMP<sup>+</sup>19].

<sup>4</sup><http://geneontology.org/>.

<sup>5</sup><https://portal.gdc.cancer.gov/>

<sup>6</sup><https://go.drugbank.com/>.

<sup>7</sup><https://www.cancer.gov/about-cancer/treatment/drugs/breast>.

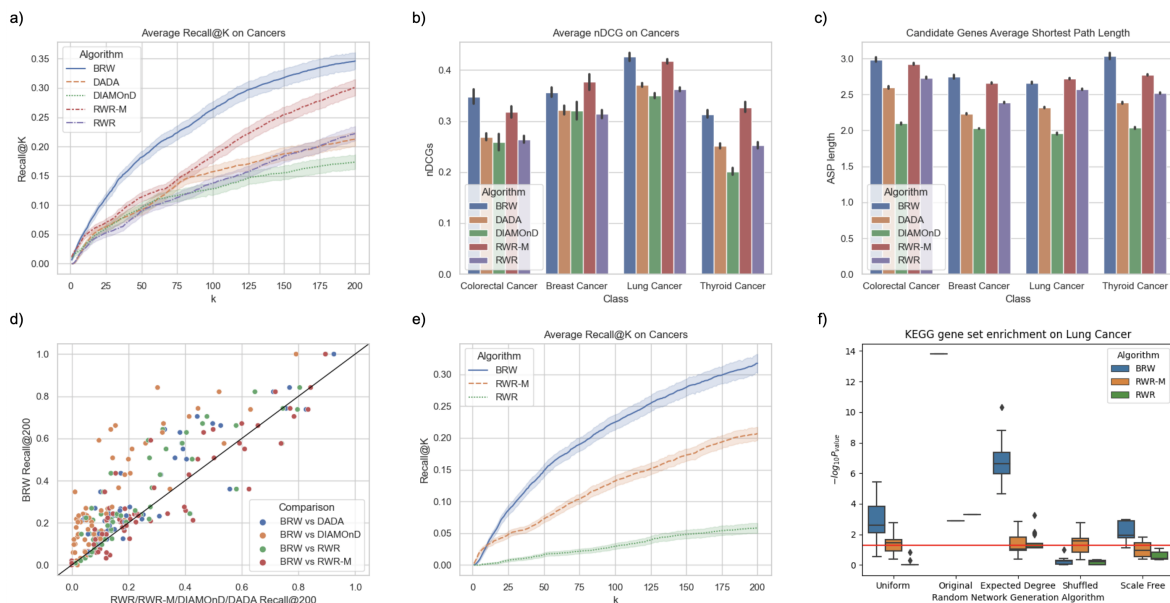


Figure 2: Algorithm comparison: a) and b) compare respectively the Recall@K and nDCG of some of well known network based approaches with BRW on four types of cancer using a 100-fold Monte Carlo random sampling validation choosing uniformly at random the 70% of known disease genes and considering the remaining ones as the test set (30%). c) shows the average shortest path length of top 200 candidates predicted by the analyzed algorithms. d) shows the comparison between BRW with the state of the art on a corpus of 70 Mendelian diseases downloaded from [GMB15]. e) compares multi-omics frameworks (BRW and RWR-M) on average Recall@k on cancer phenotypes when the PPI network is randomized. The average Recall@K is computed as described in the previous experiment. f) illustrate how multi-omics integration affect the bias induced by curated ontologies such as GO, Kegg, and Reactome and the PPI network. It compares the distribution of p-values (negative log scale) computed by the testsuit using KEGG pathways and **gseapy** on gene sets predicted on randomized PPI networks with those predicted on the original PPI. As hypothesized, BRW, having in input statistical significant pathways from KEGG, Reactome, and GO, returns biologically meaningful candidate sets. However, their significance is not comparable with the set predicted using the original PPI.

**Performance indices.** We used the widely adopted indices Recall@K and nDCG in some of the experiments described in the remainder. To keep presentation self-contained, they are briefly described in Section C.1 of the supplementary material.

### 3.2 Multi-Omics Integration Improves Algorithm performance

In a first round of experiments, we performed two (internal) validation steps: i) we first compared the algorithms with respect to four cancer phenotypes (i.e, breast cancer, lung adenocarcinoma, papillary thyroid cancer, colorectal adenocarcinoma), for which both biological annotations and gene expression data are available; ii) as a further step, we performed a broader, yet less specific validation on a corpus of 70 manually curated mendelian diseases [GMB15], for which only biological annotations were used. For each disease, we performed a mean 100-fold validation, by sampling 70% of known disease genes uniformly at random and using the rest to test the algorithms. For each tested disorder, we computed Recall@K and the nDCG of each algorithm.

**Four cancer phenotypes.** We performed a grid search to identify the best combination of hyper-parameters ( $\alpha, \beta, r$ ). The benchmark, discussed in Section C.2 of the supplementary material and illustrated in Supplementary Fig. 6 and Supplementary Fig. 7, highlights interesting, mixed results. For the task of disease gene prioritization<sup>8</sup> and to the purpose of computing personalization vectors

<sup>8</sup>We remark that the settings discussed here are not optimal for other tasks in general, e.g., drug target discovery (see Section 3.4).

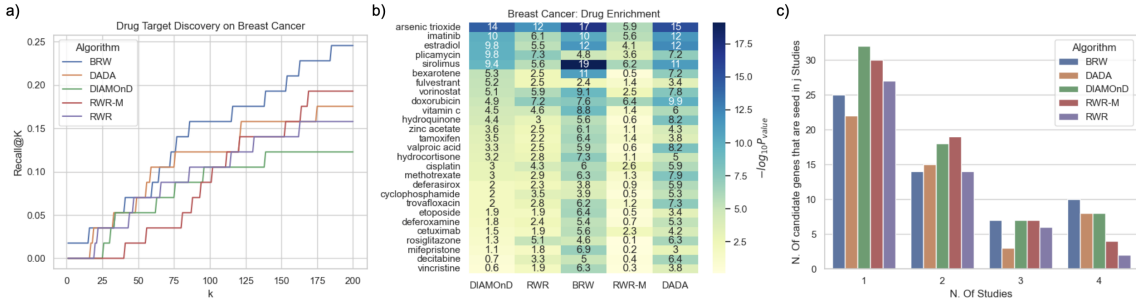


Figure 3: **Algorithm Comparison on Breast Cancer Disease:** a) percentage of Breast Cancer Drug targets found by each framework in the top K positions. b) drugs that are enriched (corrected p-value  $\leq 10^{-5}$ ) in at least one of the predicted candidate gene sets. c) number of candidate genes, predicted by each algorithm, that are frequently mutated in at least j of the remaining studies, with  $j \in \{1, 2, 3, 4\}$ .

(i.e., teleporting probabilities), the signal contained in statistically significant annotations derived from seed genes is definitely stronger than the signal carried by gene expression, so that the best choice for disease gene prioritization on cancer phenotypes is  $\alpha = 1.0$ , thus completely removing information about differentially expressed genes. However, gene expression information is crucial in determining the transition matrix of the random walk, with values of  $\beta \in [0.25, 0.5]$  achieving best predictive performance, indicating that both information sources provide crucial information to BRW for disease gene ranking.

Results for the four cancer phenotypes show that algorithms that only leverage the PPI tend to perform worse in terms of both Recall@k and nDCG, as shown in figure 2 a) and 2 b). Conversely, multi-Omics methods that, like BRW and RWR-M, rely on multiple biological information sources typically perform better in terms of the aforementioned indices. Improvement of these methods over single-source baselines at least in part stems from the well-known fact that disease-associated genes tend to be involved in similar pathways and biological processes [BGL11], see also Section 3.3. Interestingly, BRW’s ability to bias the random walk towards related genes that do not necessary belong to the seed set seems to play an important role in improving prioritization of the test set, at least in terms of Recall@k. At the same time, RWR-M achieves similar performance (slightly better or worse, depending on the dataset) if one considers nDCG as a global measure of rank, as shown in figure 2 b). As previously remarked, biased teleporting makes BRW explore areas of the PPI network that could be relatively far from the seed set, a fact that is reflected in its candidate genes in the top 200 positions having higher average shortest path distance than other RWR-based methods that only teleport to genes of the seed set, as shown in Figure 2 c).

**Mendelian diseases.** As a further internal validation, we provided a less specific yet broader, comparative assessment of BRW, by performing a Monte Carlo cross-validation [DGB07] on “gold standard” gene sets. These sets contain known genes associated with 70 diseases, which were previously selected in [GMB15] from OMIM and PheGenI databases. As discussed more in detail at the end of Section A.1, in this experiment (and only in this one) we used the PPI considered in [GMB15], for the sake of consistency.<sup>9</sup> In this second round of experiments, we set  $\alpha = 1.0$  and  $\beta = 1.0$ , since gene expression is not used. Figure 2 d) compares the performances of RWR, DIAMOnD, DADA, RWR-M and BRW in terms of Recall@k. Our heuristic ranks more known disease proteins than DIAMOnD in the top 200 positions for 95 percent of disorders analyzed and respectively for 72, 73, and 63 percent of the disorders for RWR, DaDA, and RWR-M.

### 3.3 Randomization and Bias

Biological Random Walks and RWR-M leverage multiple data sources. As a result, we expect their results to be less affected by random noise in the PPI with respect to other heuristics. To test this hypothesis, we performed a first experiment, by performing an internal validation as done in Section

<sup>9</sup>All other experiments use the more recent HIPPIE-v2.2 PPI network of [ALANS16].



3.2, but this time running the random walk-based heuristics using degree-preserving randomized version of the PPI. To this purpose, we implemented the degree-preserving randomization algorithm of [MKI<sup>+</sup>03], also described in Section B.5 of the supplementary material. As hypothesized (Fig. 3 e)), by leveraging multiple biological sources, BRW and RWR-M are less affected by randomization of the PPI. This effect is stronger in BRW, whose teleporting probabilities also depend on phenotype information (statistically significant ontologies, pathways, and differentially expressed genes). This is further shown in the more detailed Supplementary Fig. 8 a) of the supplementary material, highlighting a positive correlation between the number of test genes ranked in the first 200 positions (Recall@K) and the value of BRW’s restart probability  $r$ . As remarked above, this effect is also present in RWR-M, in which heterogeneous biological sources are summarized in different, layered networks. In particular, as shown in Supplementary Fig. 8 a) of the supplementary material, RWR-M’s performance degrades significantly if one also randomizes the Pathways network used by the algorithm. Altogether, these results suggest that phenotypical information associated to the nodes plays an important role in prioritization for these heuristics, owing to the fact that known disease proteins tend to be involved in the same pathways, a fact that becomes apparent in an internal-only validations as the one considered in this section.

The results above are part of a more general phenomenon. As shown in [LBLB21], several heuristics inherit biases present in up-to-date PPI networks and manually curated ontologies such as GO, KEGG, and Reactome, in some cases with results that improve when the PPI is replaced by a randomized one. To further investigate this issue, in particular, the bias inherited by BRW when ontologies from manually curated data sources are used, we considered the AMIM (Active Module Identification Methods) test suite proposed in [LBLB21], which allows systematic comparison of candidate gene sets predicted using an original PPI network and perturbed versions thereof. To this purpose, we considered the Lung Cancer phenotype, which was both considered in Section 3.2 and is used as a benchmark in [LBLB21]. We considered randomized versions of the original PPI obtained using all randomization algorithms implemented in the test suite (i.e., expected degree, uniform, shuffled and scale-free). Candidate genes ranked by BRW, RWR-M, and RWR using the original PPI as input were compared with the results obtained using each of the aforementioned randomized counterparts of the PPI. Statistical significance was computed on KEGG pathways enrichments computed by the test suite on predefined KEGG pathway.

Fig. 2 f) shows that BRW, RWR-M, and RWR extract statistically significant candidate gene sets on the original PPI network. Relying only on the PPI, RWR provides no statistically significant results when the PPI is randomized, except when expected degree is preserved.<sup>10</sup> On the other hand, BRW and RWR-M inherit PPI and ontology’s biases, so that their results are still statistically significant when the PPI is randomized using expected degree, scale-free and uniform randomization algorithms. Still, BRW’s results are considerably more significant when the original network is used, indicating that topology of the PPI is crucial to (more) effectively propagate information extracted from other biological sources. BRW predicts more significant outcomes on the actual PPI than on the randomized versions. While all ontologies (GO, KEGG, and Reactome) were considered in the experiment summarized in Fig. 2 f), we further investigated BRW’s behaviour when KEGG (which is used in the enrichment) is not used. In this case, BRW’s results are no longer statistically significant if one randomizes the network, with the exception of a mild significance when expected degree is preserved (see again footnote 10 for an explanation).

### 3.4 A Case Study: Breast Cancer Phenotype

In this section, we discuss the results of an in-depth analysis of BRW’s performance on the Breast Cancer phenotype, a global health concern [SMJ<sup>+</sup>14, CRA<sup>+</sup>21], with 284,200 new cases and more than 44,000 deaths in the USA in 2021 [SMJ<sup>+</sup>14]. In particular, we present i) an external validation using drugs FDA approved drugs; ii) Drug enrichment; iii) an assessment of the algorithm(s) stability across multiple populations.

<sup>10</sup>This phenomenon arises because the stationary distribution of a random walk on an undirected network follows exactly the degree distribution. As a result, the stationary distribution of a random walk with restart over an undirected network is positively correlated with degree distribution.

### 3.4.1 Drug Target Discovery

We validated the top candidate gene sets prioritized by each algorithm along different axes. To this purpose, we created a test set of target genes for Breast Cancer drugs approved by the FDA as described in Section 3.1. Results are summarized in Figure 3 a), showing Recall@K for the algorithms we considered. Compared to other baselines, BRW prioritizes the highest number (25%) of drug targets in the top 200 candidates. Looking at the specific gene targets predicted by the algorithms, BRW predicts the highest number of genes (14 out of the 20 predicted genes), making four unique predictions, namely, Cyclin Dependent Kinases 4 and 6 (*CDK4*, *CDK6*), the Protein Kinase C Zeta (*PRKCZ*) and Caspase 3 (*CASP3*). On the other hand, the DNA Topoisomerase II Alpha (*TOP2A*) and the progesterone receptor (*PGR*) genes are uniquely predicted by DIAMOnD. The Protein Kinase C Theta gene (*PRKCQ*) is only predicted by RWR-M algorithm. More details are given in Supplementary Table 5.

Furthermore, we validated the prioritized genes from a different perspective: we considered the group of drug targets returned by each framework and showed the drugs that target them. We filtered out drugs in Drug Bank that were not annotated with the "Breast Cancer" or related associated condition. Supplementary Table 3 shows how the number of drugs ranges from 6 to 17 as we change the combination of hyper-parameters. As expected, the number of drugs correlates positively with the predicted drug target percentage (Recall@200). Supplementary Table 4 shows the drugs prioritized (i.e., a drug with at least one drug target prioritized in the top 200 positions) by BRW and the other algorithms. BRW prioritizes the highest number of drugs. Interestingly, CDK4/6 inhibitors palbociclib, ribociclib, and abemaciclib, currently used to treat hormone receptor-positive/HER2-negative metastatic breast cancer [DFF+21], are only predicted by BRW.

Finally, we identified drugs that have an enrichment with the top candidates genes predicted by each algorithm. To identify enriched drugs, we used the **gseapy** package for gene set enrichment analysis [STM+05], and we chose drugs that were enriched by at least one algorithm with a corrected p-value lower than  $10^{-5}$ . In particular, Supplementary Table 3 shows how the enrichment is affected by various hyper-parameters combinations. In this case, drug enrichment correlates positively with gene expression, and the best combination is obtained when  $\alpha$  and  $\beta$  are equal to 0.25. Indeed, while drugs target and inhibit genes involved in disease-specific pathways, the effect of the drugs can be measured by the differential expression and the co-expression between targets and nearby genes [CMP+17]. In general, results highlight the following trends: i) different biological sources (in our case, gene expression and ontologies) provide complementary information, with different subsets of FDA approved drug targets significantly enriched for both low (gene expression bias) and high (ontologies bias) values of the parameters  $\alpha$  and  $\beta$ ; ii) best performance is achieved for lower values of the restart probability  $r$  (0.25), confirming that BRW's prioritization depends on information that is not necessarily confined to the immediate neighbourhood of the seed set.

Fig. 3 b) highlights drugs that are enriched in BRW and in the other baselines considered in this manuscript, with details for each drug reported in Supplementary Table 6. Interestingly, 11 FDA-approved drugs for breast cancer treatment are enriched in BRW gene candidates (i.e., fulvestrant, doxorubicin, paclitaxel, tamoxifen, methotrexate, letrozole, cyclophosphamide, trastuzumab, fluorouracil, gemcitabine). The mTOR inhibitor sirolimus showed the best significance. While it is not currently used to treat breast cancer, preclinical *in vivo* studies demonstrated its potent antiangiogenic activity on breast cancer models [MSTDJ+22]

### 3.4.2 Breast Cancer - Multi Population Study

A desirable property of disease gene prioritization should be a certain stability in the set of proposed disease gene candidates across different populations. In other words, to some extent (e.g., up to intrinsic biases or qualitative differences in the datasets used), results should not overly depend on the specific dataset the algorithm is analyzing. To investigate this aspect, we characterized the behaviors of BRW and the other baselines we considered when applied to different population studies on Breast Cancer. We considered Invasive Breast Cancer population studies retrieved from cBioPortal datasets [STD+12, SRG+12, BCRE+12, KDK+18, CGB+15] (see Section A of supplementary material), which allowed us to identify five different seed sets for the algorithms we considered, one per study. Figure 3 d) plots the number of candidate genes, predicted by each algorithm, that are seeds in at least  $j$  other studies (frequently mutated genes in the associated populations, i.e. mutation frequency  $i$ , 1%),

for  $j \in \{1, 2, 3, 4\}$ . Notably, BRW has the highest number of candidates that are frequently mutated in the other 4 studies (the far right blue bar). The 10 genes identified by BRW, that are frequently mutated in 4 out of the 5 breast cancer populations are *AR*, *JUN*, *STAT3*, *NOTCH1*, *JAK2*, *HDAC1*, *SMAD4*, *YAP1*, and *CHD4*. While the Histone Deacetylase 1 (*HDAC1*) is also retrieved by all the other algorithms, *SMAD4* and *CHD4* are only predicted by BRW. The remaining genes are returned by BRW and at least another heuristic. Details are reported in Supplementary Table 7.

## 4 Discussion

Guided by the hypothesis that disease causing genes often share important common biological processes and pathways, we extended the random walk with restart approach to disease gene prioritization, proposing a framework that allows seamless integration of multiple biological information sources. The proposed approach consists of two main steps: i) extracting significant disease features from disease-term association data, such as statistically significant biological processes and pathways, and ii) using these features to bias the random walk with restart in a way that is consistent with the biological sources used. These two aspects are discussed in Section 2.

In general, BRW outperforms, in terms of standard indices of predictive accuracy such as recall and nDCG, previous frameworks that only rely on a single biological source, such as Random Walks with Restart [NK10], DaDa [EBEK11] and DIAMOnD [GMB15] that rely on Protein-Protein Interaction network. This is also true for an extension of RWR, namely, RWR-M [VTN<sup>+</sup>19], that performs a random walk on a multi-layer network. Using a Monte Carlo random sampling validation, we showed that prioritization results returned by BRW frequently outperform other baselines on four different cancer types: Breast, Colorectal, Lung, and Thyroid cancer. These results were further supported by a broader, computational validation on a corpus of seventy Mendelian disease manually curated by [GMB15].

A main aim of precision medicine is to use disease genes to enable tailored treatments. In this perspective, we investigated how the candidate genes prioritized by each framework are related to Breast Cancer drug targets. Results show that BRW prioritizes the highest number of drug targets in the top 200 candidates (Figure 3a). As a further assessment, we considered the group of drug targets returned by each algorithm and identified the drugs that target them. We found that BRW prioritizes the highest number of FDA-approved drugs for Breast Cancer treatment (Supplementary Table 4). In general, we noticed that drug targets are more correlated with phenotypic pathways, while drug enrichment highlights how drugs affect gene expression in terms of co-expression and differential expression. This is not surprising: indeed, although drugs often target and inhibit genes involved in disease-specific pathways, the effect of the drugs can be measured by the differential expression and the co-expression between targets and nearby genes [CMP<sup>+</sup>17].

To investigate the stability of the proposed disease gene candidates, we characterized the behaviors of BRW and the previous frameworks across different population studies. We selected “invasive breast cancer” as a phenotype and we retrieved data for 5 different populations from cBioPortal (<https://www.cbioportal.org/>). Consistently, BRW showed excellent stability, with the highest number of gene candidates in one study that are frequently mutated in the other four (Figure 3 c), Supplementary Table 7).

The BRW framework is not without limitations. On one hand, inducing a bias in teleporting probability and the transition matrix through the use of ontologies improves predictive accuracy of the algorithm. On the other hand, this bias can hinder BRW’s ability to identify new disease-related pathways. For this reason, we believe it is important to exploit the framework’s ability to integrate heterogeneous, hopefully complementary, data sources. Furthermore, experiments summarized in Fig. 7 and Supplementary Table 3 quantitatively showed that every data source comes with its bias. As a result, the relative weights attributed to different biological information sources (the combined choice of  $\alpha$  and  $\beta$  in our case) can significantly affect predictive accuracy, with a magnitude that in general depends on the validation test used. For example, while ontologies showed most effective in a computational validation and for drug target discovery, gene expression proved particularly useful in identifying a candidate gene set that is highly enriched in breast cancer and cancer related drugs. In our opinion, these results provide support to the use of (at least partially) complementary sources of biological information, even though these sometimes present non-negligible correlations, as discussed in Section 3.3.

We also emphasize that, in this study, we only leveraged a limited set of disease-specific data sources (co-expression and differential expression). Potential performance improvements might be achieved by integrating further disease information sources, such as methylation data, microRNA expression, or microRNA-target gene associations. Doing this might provide further insights into key biological mechanisms and provide new prospective gene targets, though, of course, only functional studies can provide the ultimate answer as to their biological role.


## 5 Funding.

Partially supported by the ERC Advanced Grant 788893 AMDROMA “Algorithmic and Mechanism Design Research in Online Markets”, the EC H2020RIA project “SoBigData++” (871042), and the MIUR PRIN project ALGADIMAR “Algorithms, Games, and Digital Markets”.

## References

- [ABG<sup>+</sup>09] I. Armean, A. Bridge, A. T. Ghanbarian, B. Aranda, B. Roechert, C. Derow, C. Leroy, H. Hermjakob, J. Kerssemakers, J. Khadake, K. van Eijk, L. Montecchi-Palazzi, M. Feuermann, M. Menden, M. Michaut, P. Achuthan, S. Kerrien, S. Orchard, S. N. Neuhauser, V. Perreau, and Y. Alam-Faruque. The IntAct molecular interaction database in 2010. *Nucleic Acids Research*, 38(1):D525–D531, 2009.
- [ABSH08] Joanna Amberger, Carol A Bocchini, Alan F Scott, and Ada Hamosh. Mckusick’s online mendelian inheritance in man (omim<sup>®</sup>). *Nucleic acids research*, 37(1):D793–D796, 2008.
- [ALANS16] Gregorio Alanis-Lobato, Miguel A Andrade-Navarro, and Martin H Schaefer. Hippie v2. 0: enhancing meaningfulness and reliability of protein–protein interaction networks. *Nucleic acids research*, page gkw985, 2016.
- [BCRE<sup>+</sup>12] Shantanu Banerji, Kristian Cibulskis, Claudia Rangel-Escareno, Kristin K Brown, Scott L Carter, Abbie M Frederick, Michael S Lawrence, Andrey Y Sivachenko, Carrie Sougnez, Lihua Zou, et al. Sequence analysis of mutations and translocations across breast cancer subtypes. *Nature*, 486(7403):405–409, 2012.
- [BGL11] Albert-László Barabási, Natali Gulbahce, and Joseph Loscalzo. Network medicine: a network-based approach to human disease. *Nature reviews genetics*, 12(1):56, 2011.
- [CACP<sup>+</sup>09] Andrew Chatr Aryamontri, Arnaud Ceol, Daniele Peluso, Gianni Cesareni, Leonardo Briganti, Livia Perfetto, Luana Licata, and Luisa Castagnoli. Mint, the molecular interaction database: 2009 update. *Nucleic Acids Research*, 38(1):D532–D539, 2009.
- [CGB<sup>+</sup>15] Giovanni Ciriello, Michael L Gatz, Andrew H Beck, Matthew D Wilkerson, Su-H K Rhie, Alessandro Pastore, Hailei Zhang, Michael McLellan, Christina Yau, Cyriac Kandoth, et al. Comprehensive molecular portraits of invasive lobular breast cancer. *Cell*, 163(2):506–519, 2015.
- [CGP<sup>+</sup>17] Debyani Chakravarty, Jianjiong Gao, Sarah Phillips, Ritika Kundra, Hongxin Zhang, Jiaojiao Wang, Julia E Rudolph, Rona Yaeger, Tara Soumerai, Moriah H Nissan, et al. Oncokb: a precision oncology knowledge base. *JCO precision oncology*, 1:1–16, 2017.
- [CIRS17] Lenore Cowen, Trey Ideker, Benjamin J Raphael, and Roded Sharan. Network propagation: a universal amplifier of genetic associations. *Nature Reviews Genetics*, 18(9):551, 2017.
- [CMP<sup>+</sup>17] Bin Chen, Li Ma, Hyojung Paik, Marina Sirota, Wei Wei, Mei-Sze Chua, Samuel So, and Atul J Butte. Reversal of cancer gene expression correlates with drug efficacy and reveals therapeutic targets. *Nature communications*, 8(1):1–12, 2017.

- [Con19] The Gene Ontology Consortium. The gene ontology resource: 20 years and still going strong. *Nucleic Acids Research*, 47(Database-Issue):D330–D338, 2019.
- [CRA<sup>+</sup>21] Edoardo Crimini, Matteo Repetto, Philippe Aftimos, Andrea Botticelli, Paolo Marchetti, and Giuseppe Curigliano. Precision medicine in breast cancer: From clinical trials to clinical practice. *Cancer Treatment Reviews*, 98, 2021.
- [CS04] Bond AT Carter SL, Griffin M. Gene co-expression network topology provides a framework for molecular characterization of cellular state. *Bioinformatics (Oxford, England)*, pages 2242–50, 09 2004.
- [CWB<sup>+</sup>10] Andrew Chatranyamonti, Andrew Winter, Bobby-Joe Breitkreutz, Chris Stark, Jennifer M. Rust, Julie Nixon, Kara Dolinski, Kimberly Van Auken, Lorrie Boucher, Michael S. Livstone, Mike Tyers, Rose Oughtred, Teresa Regul, Xiaodong Wang, and Xiaoqi Shi. The biogrid interaction database: 2011 update. *Nucleic Acids Research*, 39(1):D698–D704, 2010.
- [DBTVOM07] Tijn De Bie, Leon-Charles Tranchevent, Liesbeth MM Van Oeffelen, and Yves Moreau. Kernel-based data fusion for gene prioritization. *Bioinformatics*, 23(13):i125–i132, 2007.
- [DFF<sup>+</sup>21] Simona Duranti, Alessandra Fabi, Marco Filetti, Rosa Falcone, Pasquale Lombardi, Gennaro Daniele, Gianluca Franceschini, Luisa Carbognin, Antonella Palazzo, Giorgia Garganese, et al. Breast cancer drug approvals issued by ema: A review of clinical trials. *Cancers*, 13(20):5198, 2021.
- [DGB07] Werner Dubitzky, Martin Granzow, and Daniel P Berrar. *Fundamentals of data mining in genomics and proteomics*. Springer Science & Business Media, 2007.
- [DHH<sup>+</sup>18] Christos Dimitrakopoulos, Sravanth Kumar Hindupur, Luca Häfliger, Jonas Behr, Hesam Montazeri, Michael N Hall, and Niko Beerenwinkel. Network-based integration of multi-omics data for prioritizing cancer genes. *Bioinformatics*, 34(14):2441–2448, 2018.
- [ea08] Abhilash et al. Human protein reference database—2009 update. *Nucleic Acids Research*, 37(1):D767–D772, 2008.
- [EBEK11] Sinan Erten, Gurkan Bebek, Rob M Ewing, and Mehmet Koyutürk. D a d a: Degree-aware algorithms for network-based disease gene prioritization. *BioData mining*, 4(1):19, 2011.
- [GMB15] Susan Dina Ghiassian, Jörg Menche, and Albert-László Barabási. A disease module detection (diamond) algorithm derived from a systematic analysis of connectivity patterns of disease proteins in the human interactome. *PLoS computational biology*, 11(4):e1004120, 2015.
- [GMP<sup>+</sup>19] Michele Gentili, Leonardo Martini, Manuela Petti, Lorenzo Farina, and Luca Becchetti. Biological random walks: Integrating heterogeneous data in disease gene prioritization. In *2019 IEEE Conference on Computational Intelligence in Bioinformatics and Computational Biology (CIBCB)*, pages 1–8. IEEE, 2019.
- [GNZ<sup>+</sup>14] Mika Gustafsson, Colm E Nestor, Huan Zhang, Albert-László Barabási, Sergio Baranzini, Sören Brunak, Kian Fan Chung, Howard J Federoff, Anne-Claude Gavin, Richard R Meehan, et al. Modules, networks and systems medicine for understanding disease and aiding diagnosis. *Genome medicine*, 6(10):82, 2014.
- [HS09] John Hardy and Andrew Singleton. Genomewide association studies and human disease. *New England Journal of Medicine*, 360(17):1759–1768, 2009.
- [JMV<sup>+</sup>19] Bijay Jassal, Lisa Matthews, Guilherme Viteri, Chuqiao Gong, Pascual Lorente, Antonio Fabregat, Konstantinos Sidiropoulos, Justin Cook, Marc Gillespie, Robin Haw, Fred Loney, Bruce May, Marija Milacic, Karen Rothfels, Cristoffer Sevilla, Veronica

- Shamovsky, Solomon Shorser, Thawfeek Varusai, Joel Weiser, Guanming Wu, Lincoln Stein, Henning Hermjakob, and Peter D'Eustachio. The reactome pathway knowledge-base. *Nucleic Acids Research*, 48(D1):D498–D503, 11 2019.
- [JW03] Glen Jeh and Jennifer Widom. Scaling personalized web search. In *Proceedings of the 12th international conference on World Wide Web*, pages 271–279, 2003.
- [Kan19] Minoru Kanehisa. Toward understanding the origin and evolution of cellular organisms. *Protein Science*, 28(11):1947–1951, 2019.
- [KBHR08] Sebastian Köhler, Sebastian Bauer, Denise Horn, and Peter N Robinson. Walking the interactome for prioritization of candidate disease genes. *The American Journal of Human Genetics*, 82(4):949–958, 2008.
- [KDK<sup>+</sup>18] Zhengyan Kan, Ying Ding, Jinho Kim, Hae Hyun Jung, Woosung Chung, Samir Lal, Soonweng Cho, Julio Fernandez-Banet, Se Kyung Lee, Seok Won Kim, et al. Multi-omics profiling of younger asian breast cancers reveals distinctive molecular signatures. *Nature communications*, 9(1):1–13, 2018.
- [KG00] Minoru Kanehisa and Susumu Goto. KEGG: Kyoto Encyclopedia of Genes and Genomes. *Nucleic Acids Research*, 28(1):27–30, 01 2000.
- [KLPK<sup>+</sup>03] A. E. Kel, B. Lewicki-Potapov, D. Karas, D.-U. Kloos, E. Fricke, E. Gößling, E. Wingerder, H. Michael, H. Saxel, I. Reuter, K. Hornischer, M. Haubrock, M. Scheer, O. V. Kel-Margoulis, R. Geffers, R. Hehl, R. Münch, S. Land, S. Rotert, S. Thiele, and V. Matys. Transfac  : transcriptional regulation, from patterns to profiles. *Nucleic Acids Research*, 31(1):374–378, 2003.
- [KSF<sup>+</sup>18] Minoru Kanehisa, Yoko Sato, Miho Furumichi, Kanae Morishima, and Mao Tanabe. New approach for understanding genome variations in KEGG. *Nucleic Acids Research*, 47(D1):D590–D595, 10 2018.
- [KSL<sup>+</sup>13] Daniel C. Koboldt, Karyn Meltz Steinberg, David E. Larson, Richard K. Wilson, and Elaine R. Mardis. The next-generation sequencing revolution and its impact on genomics. *Cell*, 155(1):27 – 38, 2013.
- [KSSF17] Tamas Korcsmaros, Maria Victoria Schneider, and Giulio Superti-Furga. Next generation of network medicine: interdisciplinary signaling approaches. *Integrative Biology*, 9(2):97–108, 2017.
- [LBLB21] Olga Lazareva, Jan Baumbach, Markus List, and David B Blumenthal. On the limits of active module identification. *Briefings in Bioinformatics*, 22(5):bbab066, 2021.
- [LP17] David A Levin and Yuval Peres. *Markov chains and mixing times*, volume 107. American Mathematical Soc., 2017.
- [MGS<sup>+</sup>17] Jörg Menche, Emre Guney, Amitabh Sharma, Patrick J Branigan, Matthew J Loza, Frédéric Baribaud, Radu Dobrin, and Albert-László Barabási. Integrating personalized gene expression profiles into predictive disease-associated gene pools. *NPJ systems biology and applications*, 3(1):1–10, 2017.
- [MKI<sup>+</sup>03] Ron Milo, Nadav Kashtan, Shalev Itzkovitz, Mark EJ Newman, and Uri Alon. On the uniform generation of random graphs with prescribed degree sequences. *arXiv preprint cond-mat/0312028*, 2003.
- [MSK<sup>+</sup>15] Jörg Menche, Amitabh Sharma, Maksim Kitsak, Susan Dina Ghiassian, Marc Vidal, Joseph Loscalzo, and Albert-László Barabási. Uncovering disease-disease relationships through the incomplete interactome. *Science*, 347(6224):1257601, 2015.

- [MSTDJ<sup>+</sup>22] Muhammad Shahidan Muhammad Sakri, Tengku Ahmad Damitri Al-Astani Tengku Din, Hasnan Jaafar, Vinod Gopalan, and Wan Faiziah Wan Abdul Rahman. Rapamycin as a potent and selective inhibitor of vascular endothelial growth factor receptor in breast carcinoma. *International Journal of Immunopathology and Pharmacology*, 36:20587384211059673, 2022.
- [NK10] Saket Navlakha and Carl Kingsford. The power of protein interaction networks for associating genes with diseases. *Bioinformatics*, 26(8):1057–1063, 2010.
- [ODC<sup>+</sup>18] Kivilcim Ozturk, Michelle Dow, Daniel E Carlin, Rafael Bejar, and Hannah Carter. The emerging potential for network analysis to inform precision cancer medicine. *Journal of molecular biology*, 2018.
- [PRASP<sup>+</sup>20] Janet Piñero, Juan Manuel Ramírez-Anguita, Josep Saüch-Pitarch, Francesco Ronzano, Emilio Centeno, Ferran Sanz, and Laura I Furlong. The disgenet knowledge platform for disease genomics: 2019 update. *Nucleic acids research*, 48(D1):D845–D855, 2020.
- [RBW<sup>+</sup>09] Andreas Ruepp, Barbara Brauner, Brigitte Waegle, Corinna Montrone, Gisela Fobo, Goar Frishman, H.-Werner Mewes, Irmtraud Dunger-Kaltenbach, and Martin Lechner. CORUM: the comprehensive resource of mammalian protein complexes—2009. *Nucleic Acids Research*, 38(1):D497–D501, 2009.
- [RHJ<sup>+</sup>14] Erin M Ramos, Douglas Hoffman, Heather A Junkins, Donna Maglott, Lon Phan, Stephen T Sherry, Mike Feolo, and Lucia A Hindorff. Phenotype–genotype integrator (phegeni): synthesizing genome-wide association study (gwas) data with existing genomic resources. *European Journal of Human Genetics*, 01 2014.
- [SCCR12] Gabriele Sales, Enrica Calura, Duccio Cavalieri, and Chiara Romualdi. g raphite-a bio-conductor package to convert pathway topology to gene network. *BMC bioinformatics*, 13(1):1–12, 2012.
- [SL20] Haixia Shang and Zhi-Ping Liu. Network-based prioritization of cancer genes by integrative ranks from multi-omics data. *Computers in biology and medicine*, 119:103692, 2020.
- [SMJ<sup>+</sup>14] Rebecca Siegal, KD Miller, Ahmddin Jemal, et al. Cancer statistics, 2012. *Ca Cancer J Clin*, 64(1):9–29, 2014.
- [SPCP10] Jan Schellenberger, Junyoung O. Park, Tom M. Conrad, and Bernhard Palsson. Bigg: a biochemical genetic and genomic knowledgebase of large scale metabolic reconstructions. *BMC Bioinformatics*, 11(1):213, 2010.
- [SRG<sup>+</sup>12] Sohrab P Shah, Andrew Roth, Rodrigo Goya, Arusha Oloumi, Gavin Ha, Yongjun Zhao, Gulisa Turashvili, Jiarui Ding, Kane Tse, Gholamreza Haffari, et al. The clonal and mutational evolution spectrum of primary triple-negative breast cancers. *Nature*, 486(7403):395–399, 2012.
- [SSA<sup>+</sup>20] Edwin K Silverman, Harald HHW Schmidt, Eleni Anastasiadou, Lucia Altucci, Marco Angelini, Lina Badimon, Jean-Luc Balligand, Giuditta Benincasa, Giovambattista Capasso, Federica Conte, et al. Molecular networks in network medicine: Development and applications. *Wiley Interdisciplinary Reviews: Systems Biology and Medicine*, 12(6):e1489, 2020.
- [STD<sup>+</sup>12] PJ Stephens, PS Tarpey, H Davies, P Van Loo, C Greenman, DC Wedge, S Nik-Zainal, S Martin, I Varela, GR Bignell, et al. Oslo breast cancer consortium (osbreac) the landscape of cancer genes and mutational processes in breast cancer. *Nature*, 486(7403):400–404, 2012.
- [STM<sup>+</sup>05] Aravind Subramanian, Pablo Tamayo, Vamsi K. Mootha, Sayan Mukherjee, Benjamin L. Ebert, Michael A. Gillette, Amanda Paulovich, Scott L. Pomeroy, Todd R. Golub, Eric S. Lander, and Jill P. Mesirov. Gene set enrichment analysis: A knowledge-based approach for interpreting genome-wide expression profiles. *Proceedings of the National Academy of Sciences*, 102(43):15545–15550, 2005.

- [VTN<sup>+</sup>19] Alberto Valdeolivas, Laurent Tichit, Claire Navarro, Sophie Perrin, Gaelle Odelin, Nicolas Levy, Pierre Cau, Elisabeth Remy, and Anaïs Baudot. Random walk with restart on multiplex and heterogeneous biological networks. *Bioinformatics*, 35(3):497–505, 2019.
- [WDG<sup>+</sup>17] David Wishart, Yannick Djoumbou, An Chi Guo, Elvis Lo, Ana Marcu, Jason Grant, Tanvir Sajed, Daniel Johnson, Carin Li, Zinat Sayeeda, Nazanin Assempour, Ithayavani Iynkkaran, Yifeng Liu, Adam Maciejewski, Nicola Gale, Alex Wilson, Lucy Chin, Ryan Cummings, Diana Le, and Michael Wilson. Drugbank 5.0: A major update to the drugbank database for 2018. *Nucleic acids research*, 46, 11 2017.
- [XL06] Jianzhen Xu and Yongjin Li. Discovering disease-genes by topological features in human protein–protein interaction network. *Bioinformatics*, 22(22):2800–2805, 09 2006.



## A Data

### A.1 Protein-Protein Interaction networks

To run the experiment presented in Section 3, we considered two different PPI networks:

1. HIPPIE-v2.2: Protein-protein interaction network downloaded from [ALANS16]. We filtered the network, keeping only the edges with a score larger than 0.7. Then, we mapped each node to its Ensembl id, removing nodes mapped on multiple Ensembl Ids. This way, we derive a PPI network with 88,865 edges and 12,148 nodes.
2. [GMB15]: We used the same Protein-Protein Interaction network (PPI) as in [GMB15]. In [GMB15], the authors only considered direct physical protein interactions with reported experimental evidence. They derive this PPI network with the help of several data sources: TRANSFAC, [KLPK+03], IntAct [ABG+09], MINT [CACP+09], BioGRID [CWB+10], HPRD [ea08] KEGG, BIGG [SPCP10], and CORUM [RBW+09]. Then, we considered the main connected component of the network and we removed self-loops (i.e., edges describing proteins' self-interactions). The resulting graph consists of 13396 nodes and 138405 edges.

**Remark.** Note that the PPI of [GMB15] was used only in the internal validation on the 70 mendelian diseases, whose results are discussed in Section 3.2 of the main article. This was done for consistency, since the network considered in [GMB15] was explicitly curated to include all genes that are associated to at least one of the 70 diseases under consideration, some of which might be missing in other, even more recent, networks. Instead, all other experiments in this paper used the more recent HIPPIE-v2.2 PPI [ALANS16].

### A.2 Biological data sources

**Gene annotations.** We used three different sources of gene biological information: Gene Ontology Consortium<sup>11</sup> where, for each gene, we downloaded its biological processes, KEGG Pathways [Kan19, KSF+18, KG00] and Reactome [JMV+19], which we used to download pathways' annotations.

**Pathways Network:** a network connecting proteins according to pathway interaction data, using the R package graphite [SCCR12].

**Tissue Network:** a co-expression network from RNA-Seq data downloaded from the Human Protein Atlas (<http://www.proteinatlas.org>) (Uhlen et al., 2015). We computed Spearman correlations of TPM (transcript per million) expression data from 32 tissues and 45 cell lines, and selected correlation having an absolute value  $\geq 0.7$  to be included in the network.

**Gene expression data (TCGA).** Gene expression datasets were downloaded from The Cancer Genome Atlas datasets.<sup>12</sup> We collected from CDC portal the RNA-Seq data of several type of cancers. Table 1 describe the cancer types downloaded and the number of Primary Tumor and Solid tissue normal used to compute the set of differentially expressed genes, and co-expression network.

Table 1: The table shows all the TCGA projects downloaded to create the set of differentially expressed genes and the CO-expression network

| Project ID | Cancer Type               | N. of Primary Tumor | N. of Solid Tissue Normal |
|------------|---------------------------|---------------------|---------------------------|
| TCGA-BRCA  | Breast Cancer             | 1077                | 99                        |
| TCGA-LUAD  | Lung Adenocarcinoma       | 519                 | 58                        |
| TCGA-THCA  | Papillary Thyroid Cancer  | 497                 | 56                        |
| TCGA-COAD  | Colorectal Adenocarcinoma | 456                 | 41                        |

<sup>11</sup><http://geneontology.org/>.

<sup>12</sup><https://portal.gdc.cancer.gov/>

| Selected Studies                  | Sanger 2012 [28]   | British 2012 [27]  | Broad 2012 [3]  | SMC 2018 [15]   | TCGA 2015 [8]   |
|-----------------------------------|--|--|---|---|---|
| N. Of subjects                    | 100 + 250  | 65   | 103   | 187   | 817   |
| Invasive Breast Cancer Histotypes | 79 ER + , 21 ER - :<br><ul style="list-style-type: none"> <li>• 76 Ductal</li> <li>• 6 Lobular</li> <li>• 9 Mixed</li> <li>• 5 Mucinous</li> <li>• 4 not available</li> </ul>              | <b>Triple Negative Breast Cancer:</b><br><ul style="list-style-type: none"> <li>• 58 Infiltrating Ductal Carcinoma</li> <li>• 4 Others</li> <li>• 1 Mixed</li> <li>• 1 Phyllodes</li> <li>• 1 not available</li> </ul> | <ul style="list-style-type: none"> <li>• 82 Infiltrating Ductal Carcinoma</li> <li>• 9 Ductal Carcinoma In Situ;</li> <li>• 4 LOBULAR</li> <li>• 3 Mixed</li> <li>• 5 Others</li> </ul> | <ul style="list-style-type: none"> <li>• 172 Ductal</li> <li>• 7 Lobular</li> <li>• 8 Others</li> </ul> | <ul style="list-style-type: none"> <li>• 490 Ductal</li> <li>• 127 Lobular</li> <li>• 88 Mixed</li> <li>• 112 Others</li> </ul>   |
| Validation Cohort                 | <b>Validation Cohort (n=250)</b><br><ul style="list-style-type: none"> <li>• 170 Ductal</li> <li>• 7 Lobular</li> <li>• 9 Mixed</li> <li>• 3 Others</li> <li>• 61 not available</li> </ul> | not available  | not available   | not available   | not available   |
| Population                        | not available  | not available  | Vietnam and New Mexico  | Asian   | <ul style="list-style-type: none"> <li>• 595 White</li> <li>• 90 Black or African American</li> <li>• 77 not available</li> <li>• 54 Asian</li> <li>• 1 American Indian or Alaska native</li> </ul> |
| Methods (retrieved data types)    | WES, (SNVs, Indels)  | WES / WGS (SNVs, Indels)   | WES / WGS (SNVs, Indels)  | WES/RNA-SEQ (SNVs, Indels, CNA, GF, GEA)  | WES/RNA-SEQ (SNVs, CNA, GF, GEA)  |

Supplementary Fig. 1: **Breast cancer studies selected from the cBioPortal for Cancer Genomics.** The table reports some details on the invasive Breast Cancer populations used in the experiments. A study was selected if it included human participants AND at least a whole exome sequencing analysis was performed (studies performing targeted sequencing analyses were ruled out) ER: Estrogen receptor, WES: Whole Exome Sequencing, WGS: Whole Genome Sequencing, SNVs: Single Nucleotide Variants, CNA: Copy Number Alteration, GF: Gene Fusions, GEA: Gene Expression Alteration

### A.3 Data sources for experimental validation

**Disease-gene associations.** We used disease-gene associations from [GMB15]. Out of a corpus of gene-disease associations involving 69 well-characterized diseases retrieved from OMIM<sup>13</sup> (Online Mendelian Inheritance in Man; [ABSH08]) and PheGenI<sup>14</sup> (Phenotype-Genotype Integrator; [RHJ+14]) databases, we focused on the **Breast Cancer** phenotype, which has associations with 40 genes.

**Disease-Gene associations of Invasive Breast Cancer on several population studies.** From cBioPortal<sup>15</sup> we downloaded Invasive Breast Cancer mutated genes belonging to 5 studies [STD+12, SRG+12, BCRE+12, KDK+18, CGB+15] (Some information about the subjects sequenced by each study is reported in Supplementary Fig. 1) and we filtered out genes mutated in less than 1% of the studied population and that are not present in the OncoKB [CGP+17]. More precisely, for each study (*reference population*), a reliable seed set was obtained, by keeping genes that i) were highly mutated in the population study under consideration (mutation frequency > 1%) and ii) were known cancer genes, present in OncoKB database [CGP+17]. At the same time, significantly mutated genes identified across the remaining four studies provided a natural validation set. Thus, for each algorithm and for each reference population, a candidate gene prioritized by the algorithm is considered to be a potential disease gene if it appears mutated gene in at least one of the other population studies. The underlying hypothesis is that genes involved in a pathological pathway are likely to be mutated in at least one population.

## B Methods

### B.1 Gene co-expression networks

At a high level, a Gene Co-expression Network (GCN) is an undirected graph, with genes as the vertices. An undirected edge exists between two nodes  $i$  and  $j$  if the corresponding genes are significantly co-

<sup>13</sup><https://www.ncbi.nlm.nih.gov/omim/>

<sup>14</sup><https://www.ncbi.nlm.nih.gov/gap/phegeni>

<sup>15</sup><https://www.cbioportal.org/>

Table 2: Breast cancer drugs filtered from DrugBank to derive a set of target genes we used to validate algorithm prediction on an external dataset.

| Drug Bank ID | Drug Name                | Target Genes                         | Drug Bank ID | Drug Name              | Target Genes  |
|--------------|--------------------------|--------------------------------------|--------------|------------------------|---|
| DB12001      | Abemaciclib              | CDK4, CDK6                           | DB05773      | Trastuzumab em-tansine | ERBB2   |
| DB01229      | Paclitaxel               | TUBB1, BCL2, MAP4, MAP2, MAPT, NR1I2 | DB09037      | Pembrolizumab          | PDCD1   |
| DB05773      | Trastuzumab em-tansine   | ERBB2                                | DB11730      | Ribociclib             | CDK4, CDK6  |
| DB01590      | Everolimus               | MTOR                                 | DB01259      | Lapatinib              | EGFR, ERBB2   |
| DB12015      | Alpelisib                | PIK3CA                               | DB01006      | Letrozole              | CYP19A1   |
| DB01217      | Anastrozole              | CYP19A1                              | DB09074      | Olaparib               | PARP1, PARP2, PARP3   |
| DB00282      | Pamidronic acid (Aredia) | FDPS, GGPS1, CASP3, CASP9            | DB00351      | Megestrol acetate      | PGR, NR3C1  |
| DB01101      | Capecitabine             | TYMS                                 | DB00563      | Methotrexate           | DHFR, TYMS, ATIC  |
| DB00531      | Cyclophosphamide         | NR1I2                                | DB11828      | Neratinib              | EGFR  |
| DB01248      | Docetaxel                | TUBB1, BCL2, MAP4, MAP2, MAPT, NR1I2 | DB09074      | Olaparib               | PARP1, PARP2, PARP3   |
| DB00997      | Doxorubicin              | TOP2A, NOLC1                         | DB01229      | Paclitaxel             | TUBB1, BCL2, MAP4, MAP2, MAPT, NR1I2  |
| DB00445      | Epirubicin               | TOP2A                                | DB09073      | Palbociclib            | CDK4, CDK6  |
| DB14962      | Trastuzumab derux-tecan  | FCGR1A, TOP1                         | DB00282      | Pamidronic acid        | FDPS, GGPS1, CASP3, CASP9   |
| DB00445      | Epirubicin               | TOP2A                                | DB09037      | Pembrolizumab          | PDCD1   |
| DB08871      | Eribulin                 | BCL2, TUBB1                          | DB06366      | Pertuzumab             | ERBB2   |
| DB01590      | Everolimus               | MTOR                                 | DB14740      | Hyaluronidase          | TGFB1   |
| DB00990      | Exemestane               | CYP19A1                              | DB12015      | Alpelisib              | PIK3CA  |
| DB00544      | Fluorouracil             | TYMS                                 | DB12893      | Sacituzumab govitecan  | TACSTD2, TOP1, FUBP1  |
| DB14962      | Trastuzumab derux-tecan  | FCGR1A, TOP1                         | DB00675      | Tamoxifen              | ESR1, ESR2, EBP, AR, KCNH2, NR1I2, ESRRG, SHBG, MAPK8, PRKCA, PRKCB, PRKCD, PRKCE, PRKCG, PRKCI, PRKCQ, PRKCZ |
| DB00539      | Toremifene               | ESR1, SHBG                           | DB11760      | Talazoparib            | PARP1, PARP2  |
| DB00947      | Fulvestrant              | ESR1                                 | DB11595      | Atezolizumab           | CD274   |
| DB01006      | Letrozole                | CYP19A1                              | DB00539      | Toremifene             | ESR1, SHBG  |
| DB00544      | Fluorouracil             | TYMS                                 | DB00563      | Methotrexate           | DHFR, ATIC, TYMS  |
| DB00441      | Gemcitabine              | RRM1, TYMS, CMPK1                    | DB12893      | Sacituzumab govitecan  | TACSTD2, TOP1, FUBP1  |
| DB00014      | Goserelin                | LHCGR, GNRHR                         | DB11652      | Tucatinib              | ERBB2, ERBB3  |
| DB08871      | Eribulin                 | BCL2, TUBB1                          | DB01259      | Lapatinib              | EGFR, ERBB2   |
| DB00072      | Trastuzumab              | ERBB2                                | DB12001      | Abemaciclib            | CDK4, CDK6  |
| DB09073      | Palbociclib              | CDK4, CDK6                           | DB00570      | Vinblastine            | TUBA1A, TUBB, TUBD1, TUBG1, TUBE1, JUN  |
| DB00441      | Gemcitabine              | RRM1, TYMS, CMPK1                    | DB01101      | Capecitabine           | TYMS  |
| DB04845      | Ixabepilone              | TUBB3                                | DB00014      | Goserelin              | LHCGR, GNRHR  |

expressed in the subject population.<sup>16</sup> Hence, differently from a PPI, a GCN is disease-specific. Intuitively, for two genes  $i$  and  $v$ , this means that the transcript levels of  $u$  and  $j$  tend to vary in a similar fashion across the subject population. Gene co-expression networks [CS04] are of biological interest since co-expressed genes tend to be controlled by the same transcriptional regulatory program, i.e., they are functionally related or members of the same pathway or protein complex.

## B.2 Biological Random Walks

### B.2.1 Overview

As we described in the main article, we compute the personalization vector  $\mathbf{q}$  and the transition matrix  $W$  by leveraging multiple biological information sources. We remind that we refer to the biological information associated to a gene  $i$  (e.g., the set of its annotations) as the set of its *features*, denoted by  $features(i)$ , such as the Gene Ontology database [Con19] (GO in the remainder) or gene expression levels and their consequently differential expression scores. BRW ranks genes according to three main steps:

1. Rather than using the standard approach<sup>17</sup>, we compute a personalization vector  $\mathbf{q}$ , *i.e.* *Biological Teleporting Probability* (BTP), associating individual teleporting probabilities to all nodes of the PPI. Qualitatively speaking, the probability of teleporting to a given node increases, the higher its feature-based similarity with the disease.
2. In a similar fashion, we derive the transition matrix  $W$  of the random walk by also leveraging biological information, whereby the probability of a transition between genes  $i$  and  $j$  tends to be higher, the more functionally closer the genes are.
3. Finally, we rank genes according to their *Biological Random Walk (BRW)* scores.

## B.3 Biological Teleporting Probability

Both annotation data and gene expression levels allow derivation of personalization vectors that reflect some notion of similarity between a gene and a disease, *i.e.* its seed genes. In the first case, this similarity is defined in terms of knowledge about genes’ involvement in various biological functions and/or diseases. In the second case, similarity is defined in terms of co-expression levels of different genes in subject cases as opposed to expression levels in a control group, using data about a population of patients involved in a clinical trial. It’s worth noting that this approach allows to easily extend the algorithm on a multiomics approach and/or tissue specific analysis, as long as it is possible to recapitulate data as a score for each gene (*i.e.* chromatin accessibility) or pair of genes (*i.e.* co-targeted by miRNA).

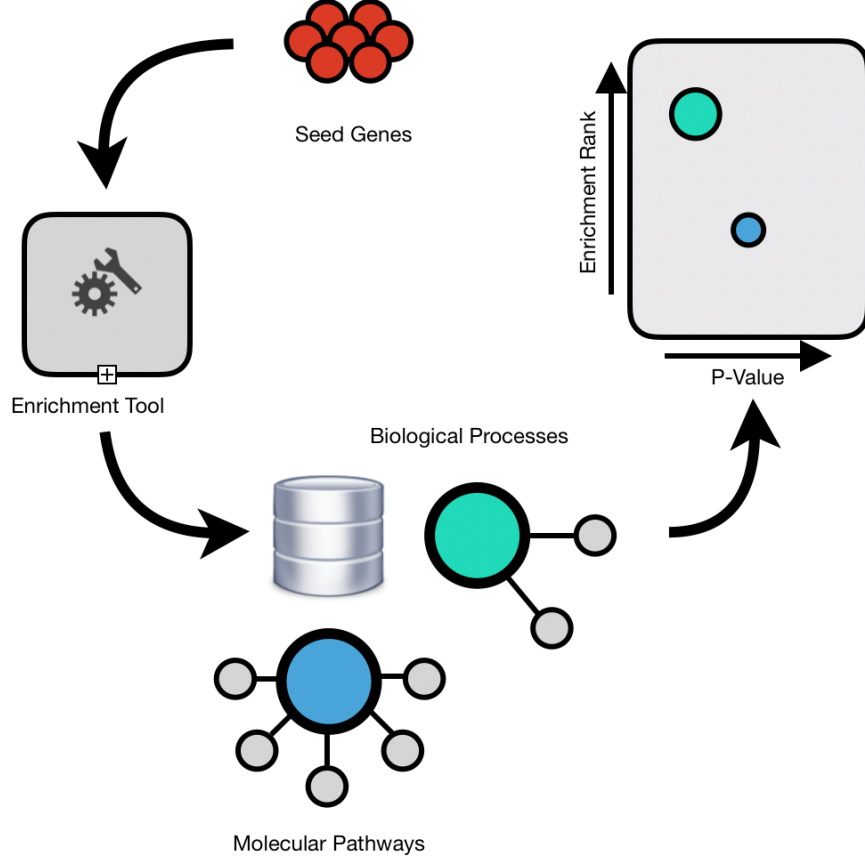
### B.3.1 Computing a Personalization Vector

Building on the hypothesis that genes involved in the same disease tend to be functionally related and thus share similar biological information, a first approach to deriving the personalization vector  $\mathbf{q}$  relies on assigning scores to genes in the PPI using biological information.

**Using Biological Information.** We assume we have  $\ell$  sources of biological information. Assume  $S$  is the seed set. for every  $j = 1, \dots, \ell$ , we use  $\mathcal{F}^j$  to denote the subset of annotations from the  $j$ -th source that are associated with at least one gene in  $S$ . Then, for every  $j = 1, \dots, \ell$ , we selected the subset of annotation  $\widehat{\mathcal{F}}^j$  filtering out the annotations that are not statistically significant as shown in Supplementary Fig.2 (i.e.,  $p$  - value  $> 10^{-5}$  using Fisher Exact Test and FDR correction) so that  $\mathcal{F} = \cup_{j=1}^{\ell} \widehat{\mathcal{F}}^j$  denotes the set of all statistically significant annotations that are associated with genes in  $S$ . Likewise, for every gene  $i$  (not necessarily belonging to  $S$ ), we denote by  $\mathcal{A}(i)$  the set of its annotations, possibly extracted from multiple biological information sources. We next assign each gene  $i$  a weight  $\theta_i$  as follows:

<sup>16</sup>In the remainder we use the same letter to denote a gene and the corresponding vertex in the PPI or GCN.

<sup>17</sup>We remind that in the standard RWR approach [KBHR08], the probability of restarting the random walk from a given seed node (disease gene) is the same for all seeds nodes, while it is 0 for other nodes of the PPI.



Supplementary Fig. 2: Enrichment step: starting from a seed set  $S$ , We filter out  $S'$  annotations that are not statistically significant using Fisher Exact Test and FDR correction.

$$\theta_i = \begin{cases} \ell & \text{if } i \in S, \\ \sum_{j=1}^{\ell} \frac{|\mathcal{A}(i) \cap \mathcal{F}^j|}{|\mathcal{F}^j|} & \text{otherwise,} \end{cases} \quad (8)$$

if we want to weigh the seed set  $S$  more than the subset of genes that are biologically similar to  $S$ . Otherwise, we can assign weights as follows:

$$\theta_i = \sum_{j=1}^{\ell} \frac{|\mathcal{A}(i) \cap \mathcal{F}^j|}{|\mathcal{F}^j|} \quad (9)$$

If no biological information is used (i.e., we are only using knowledge of whether a given gene belongs to the seed set or not like in [KBHR08]), each gene  $i$  is assigned a weight  $\theta_i$  as follows:

$$\theta_i = \begin{cases} 1 & \text{if } i \in S \\ 0 & \text{otherwise} \end{cases} \quad (10)$$

At this point, components of a personalization vector  $\mathbf{q}$  can be computed as follows:

$$q_i = \frac{\theta_i}{\sum_{i=0}^N \theta_i}, \quad (11)$$

with  $N$  the number of genes we consider. Note that  $q_i$  denotes the probability that, upon teleportation, the random walkers jumps to gene  $i$ .

**Using gene expression data.** RNA sequencing techniques have changed our ability to explore the molecular mechanisms underlying complex diseases and they have been used to identify potential disease-associated genome-wide changes in gene expression patients. An important goal is the identification of Differentially Expressed (DE) genes, whose expression levels systematically differ between case (Breast Cancer tissues) and a control group (Healthy Breast tissues).

We take inspiration from the framework to construct and integrate personalized perturbation profiles (PEEPs) from gene expression data proposed in [MGS<sup>+</sup>17], to derive gene expression-aware personalization vectors.

PEEPs turn individual expression heterogeneity into a predictive information by constructing personalized perturbation profiles that reflect expression changes within a single subject. For each gene  $i$  and for each subject  $j$ , the expression level  $l_i^j$  is compared with the distribution of the expression level of gene  $i$  within the control group. This comparison is measured by the corresponding  $z$ -score, defined as:

$$z_{ij} = \frac{l_i^j - \mu_i}{\sigma_i}, \quad (12)$$

where  $\mu_i$  and  $\sigma_i$  respectively denote the mean and the standard deviation of gene  $i$ 's expression level in the control group. This approach allows association of a "bar code" [MGS<sup>+</sup>17] to each subject, thus allowing to tell differentially expressed genes ( $|z_{ij}| > 2.5$ ) from regular ones.

In general, given a case and a control group, it is possible to build a matrix  $Z \in R^{n \times m}$ , where  $n$  and  $m$  are respectively the number of genes and subjects:

$$Z = \begin{bmatrix} z_{11} & z_{12} & \cdots & z_{1m} \\ z_{21} & z_{22} & \cdots & z_{2m} \\ \vdots & \vdots & \ddots & \vdots \\ z_{n1} & z_{n2} & \cdots & z_{nm} \end{bmatrix} \quad (13)$$

Thus, we might consider only one gene and subject at time, or we might consider a gene  $i$  as the vector  $Z_i$  of the  $z$ -scores of its expression levels in the subject group. This provides an overall description of how gene  $i$ 's expression varies within the case group.

Using matrix  $Z$ , we identify the subset of genes that are differentially expressed in the subject group as follows. In particular, we define a new binary matrix  $\hat{Z}$  which, for each gene  $i$  and patient  $j$ , specifies whether or not  $i$  is differentially expressed in subject  $j$ . Following [MGS<sup>+</sup>17], we assume this to happen when its  $z$ -score  $z_{ij}$  exceeds 2.5 standard deviations. Namely:

$$\hat{Z}_{ij} = \begin{cases} 1 & \text{if } |z_{ij}| > 2.5 \\ 0 & \text{otherwise} \end{cases} \quad (14)$$

Next, a gene  $g$  is considered to be *differentially expressed* in the subject group if the number of patients in which it is differentially expressed according to the above definition exceeds the mean:

$$\sum_j \hat{Z}_{gj} > \frac{1}{n} \sum_i \sum_j \hat{Z}_i^j. \quad (15)$$

The subset of differentially expressed genes this identified can be used to define a personalization vector  $\mathbf{q}$ , using the PPI to identify differentially expressed genes that are also close to known disease genes (seeds) in the PPI. In particular, we obtain a personalization vector according to the following criteria: i)  $\mathbf{q}_i$  is non-zero only for differentially expressed genes; ii)  $\mathbf{q}_i$  increases with the number of disease genes in the vicinity of  $i$ . In particular, for a differentially expressed gene  $i$ , we define a score  $\phi_i$  as the proportion of its neighbors within shortest path distance 2 that are disease proteins [XL06], namely:

$$\phi_i = \frac{|N(i) \cap S|}{N(i)} + \frac{|N_2(i) \cap S|}{N_2(i)} \quad (16)$$

where we remind that  $S$  denotes the seed set in the random walk with restart. Finally, scores are normalized to obtain restart probabilities, so that:

$$\mathbf{q}_i = \frac{\phi_i}{\sum_{i=0}^N \phi_i} \quad (17)$$

### B.3.2 Integrating Biological Information and Gene Expression

We discussed above two orthogonal approaches to the design of personalization vectors. The first one leverages similarities between the biological processes associated to known disease proteins and those to be prioritized. Hence, teleporting probabilities depend on the seed set through association with common biological processes.

In the second case, teleporting probabilities depend on information that is tissue-specific (the level of expression in a population of subjects affected by a certain disease) and partly on the seed set, but this time through the PPI’s topology. Hence, these two approaches largely rely on complementary sources of information. In the following paragraphs, we discuss ways to integrate these complementary sources into a unique personalization vector that leverages both.

Assume we have computed two personalization vectors  $\mathbf{q}_1$  and  $\mathbf{q}_2$ , the former using biological information only, the latter using gene expression data and the PPI.

A first approach to integrating them is considering a convex combination, namely:

$$\mathbf{q} = \alpha\mathbf{q}_1 + (1 - \alpha)\mathbf{q}_2, \quad (18)$$

where  $\alpha \in [0, 1]$ . Parameter  $\alpha$  allows to weigh the importance of the different information sources we are using. In our experiments, we set  $\alpha = 1/2$ . Intuitively, this type of aggregation amounts to considering a gene a potential candidate if it is statistically significant in terms of its involvement in biological processes, gene expression levels in the subject group, or both.

**Remark.** Despite its simplicity, this is a mathematically principled choice. In particular, it is well-known [JW03] and easy to show that the stationary distribution corresponding to the convex combination of two personalization vectors  $\mathbf{q}_1$  and  $\mathbf{q}_2$  is itself the linear combination of the stationary distributions corresponding to  $\mathbf{q}_1$  and  $\mathbf{q}_2$  respectively. Briefly put, the parameter  $\alpha$  allows us to tune the relative importance of the information provided by gene annotations and gene expression levels respectively. Moreover, this approach extends seamlessly to an arbitrary number of heterogeneous sources of information (and corresponding personalization vectors).

Alternatively, we can consider a gene to be a potential candidate if it is statistically significant both in terms of the biological processes it is involved in (with respect to the seed of known disease genes) and of its expression levels in the population of subjects. In this case, a natural way to define  $\mathbf{q}$  is as follows:

$$\mathbf{q}_i = \frac{\mathbf{q}_{1i} \cdot \mathbf{q}_{2i}}{\sum_{j=1}^n \mathbf{q}_{1j} \cdot \mathbf{q}_{2j}}. \quad (19)$$

Note that, again,  $\mathbf{q}$  is a probability distribution over the genes.

## B.4 Biological Transition Matrix

### B.4.1 Computing a Transition Matrix

Similar approaches can be used to derive a transition matrix for the random walk with restart. Both approaches rely on the PPI, differing on the way PPI’s edges are assigned weights that reflect genes’ similarity and determine the probabilities of edge traversals.

### B.4.2 Using Biological Information

In this case, we consider a weighted transition matrix  $W$ , in which each entry  $W_{ij}$  depends on the extent to which nodes genes  $i$  and  $j$  of the PPI share common annotations (i.e., they are involved in common biological processes) that are also significant for the disease. In more detail, considered genes  $i$  and  $j$ , we define the following *Disease Specific Interaction Function* (DSI function in the remainder):

$$DSI(i, j) = |\mathcal{A}(i) \cap \mathcal{A}(j) \cap \mathcal{F}|, \quad (20)$$

where we remind that  $\mathcal{A}(k)$  denotes the set of gene  $k$ ’s annotations, while  $\mathcal{F}$  denotes the overall set of annotations that are statistically significant for disease genes.

Intuitively, the higher  $DSI(i, j)$ , the more  $i$  and  $j$  share annotations that are also statistically significant for the disease under consideration.

In the end, edges in the PPI will be assigned weights depending on the DIS function as follows:

$$W_{ij} = \begin{cases} c + DSI(i, j) & \text{if } (i, j) \in E, \\ 0 & \text{otherwise.} \end{cases} \quad (21)$$

Here,  $c$  is a positive constant that accounts for usual sparsity of the available datasets, so that no biological information may be available for the end-points of a link in the PPI. In this case, the link receives a minimum weight  $c$ .

### B.4.3 Using Co-Expression Information

In this case, we use gene expression information about a population of patients, in order to augment the PPI with tissue-specific information. Specifically, gene expression information is used to assign weights to edges, this time reflecting similarities between genes in terms of co-expression with respect to the subject population.

Consider a CO-Expression network in which each pair of gene  $(i, j)$  is associated a score defined by the Pearson’s correlation coefficient  $pc_{i,j}$ . We need  $pc_{i,j}$  to be a probability distribution on PPI network for each gene  $i \in V$ . Thus, we define the probability of the random walker to go from node  $i$  to one of its neighbors  $j$  in the PPI network as:

$$W_{ij} = \frac{pc_{ij}}{\sum_{k \in N(i)} pc_{ik}} \quad (22)$$

where  $N(i)$  is the set of  $i$ ’s neighbors in the PPI network.

### B.4.4 Computing an Aggregate Transition Matrix

In the previous sections, we have seen how we can derive random walk’s transition matrices using only information about biological processes (i.e., annotations) or gene expression data from a population of subjects. While similar approaches apply to other prospective information sources, we show below how transition matrices derived from the aforementioned sources can be integrated into an *aggregate transition matrix*, leveraging both information sources.

Assume we have computed transition matrices  $W_1$  and  $W_2$  using biological and gene expression information respectively. We proceed in a way that is similar to the approach used to derive an aggregate personalization vector.

A first approach is considering a convex combination. Namely, for  $\beta \in [0, 1]$ , we shall consider the transition matrix

$$W = \beta W_1 + (1 - \beta) W_2.$$

Note that choosing  $\beta = 1$  corresponds to only considering biological annotations, whereas  $\beta = 0$  corresponds to only leveraging gene expression data. So,  $\beta$  is a parameter, whose tuning allows us to weigh the importance of one source of information with respect to the other. This approach can be extended to the case of more than two information sources in the obvious way.

## B.5 Network Randomization

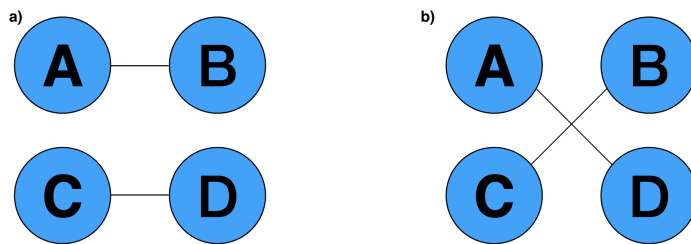
For the sake of completeness, in this section, we succinctly describe the degree-preserving, network randomization algorithm proposed in [MKI+03]. Given an initial network  $G(V, E)$ , the algorithm involves carrying out a series of Monte Carlo switching steps whereby a pair of edges  $(A \rightarrow B, C \rightarrow D)$  is selected at random and the ends are exchanged to give  $(A \rightarrow D, C \rightarrow B)$ .

Supplementary Fig. 3 shows the original edges and the switched edges after one step of the Markov Chain Monte-Carlo Switching Algorithm. However, the switching phase is not performed in two different cases:

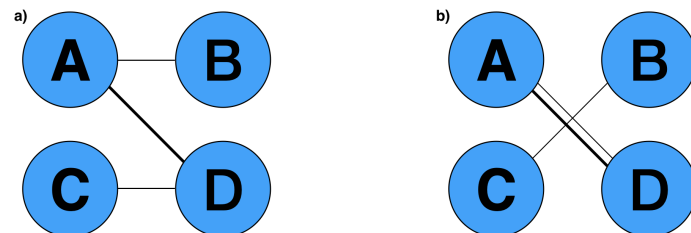
- If it generates multiple edges. For instance if it chooses the pair of edges  $(A \rightarrow D, C \rightarrow D)$  a duplicate edges is created as shown in figure 4.
- If it generates self-edges. If it randomly select the pair of edges  $(B \rightarrow A, A \rightarrow C)$ , a self-loop is created as show in figure

The entire process is repeated exactly  $Q \cdot |E|$  times, where  $E$  is the number of edges in the original network and  $Q$  is chosen large enough to have a good mixing.





Supplementary Fig. 3: Randomization process: **a)** shows the original edges in the network. **b)** shows the edges computed after the switching phase



Supplementary Fig. 4: Multiple edge generation: **a)** shows the original edges in the network. **b)** shows the duplicated edge computed after the switching phase

## C Results

### C.1 Performance indices

To assess accuracy in disease gene prioritization, for each disease analyzed, we used a 100-fold random validation approach, with each random split consisting of a training set of seed genes (corresponding to 70% of the total) that were provided as input to the algorithms and a test set, accounting for the remaining 30% of the known disease genes . To evaluate the power of each heuristic, we considered two standard prediction indices in Data Mining:

- **Recall@k:** this is the fraction of the test set that is successfully retrieved in the top  $k$  positions of the ranking computed by the algorithm.
- **nDCG:** The normalized Discounted Cumulative Gain (nDCG) is proven to be able to select the better ranking between any two, substantially different rankings. For binary classification the nDCG is given by:

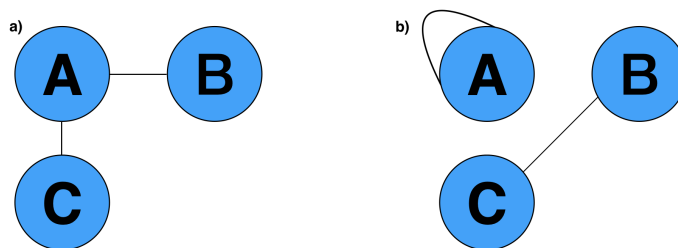
$$\frac{\sum_{i \in P} \frac{1}{\log_2(i+1)}}{\sum_{i=0}^{|P|} \frac{1}{\log_2(i+1)}}$$

Where summation in the numerator runs over all positive instances, while summation in the denominator quantifies the ideal case, in which positive instances appear in the top positions of the algorithm's ranked list.

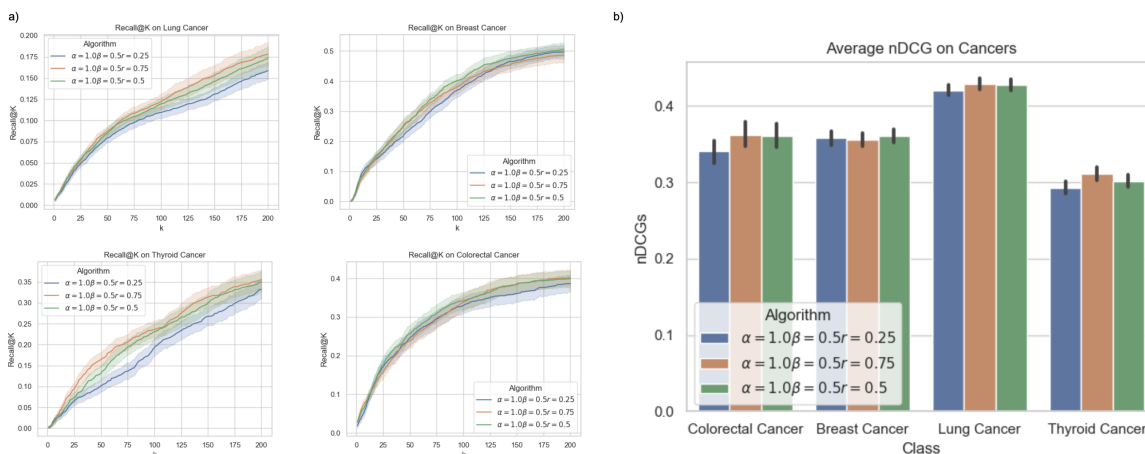
### C.2 Multi-Omics Integration

To identify the best combination of hyper-parameters, we tested how different integration approaches affect BRW's performances on the same validation benchmark discussed in the main article, in terms of Recall@k and nDCG. In more detail, we considered 3 different validation approaches: i) Monte Carlo Random Sampling, ii) Drug Target Discovery and iii) Drug Enrichment.

**Monte Carlo Sampling.** We considered all cancer phenotypes analyzed in the main article, and for each phenotype we considered different values of  $\alpha$  and  $\beta$ , fixing the restart probability  $r$  to 0.5 in order to reduce grid search space. We found out that manually curated disease genes have



Supplementary Fig. 5: Multiple edge generation: **a)** shows the original edges in the network. **b)** shows the self-loop computed after the switching phase

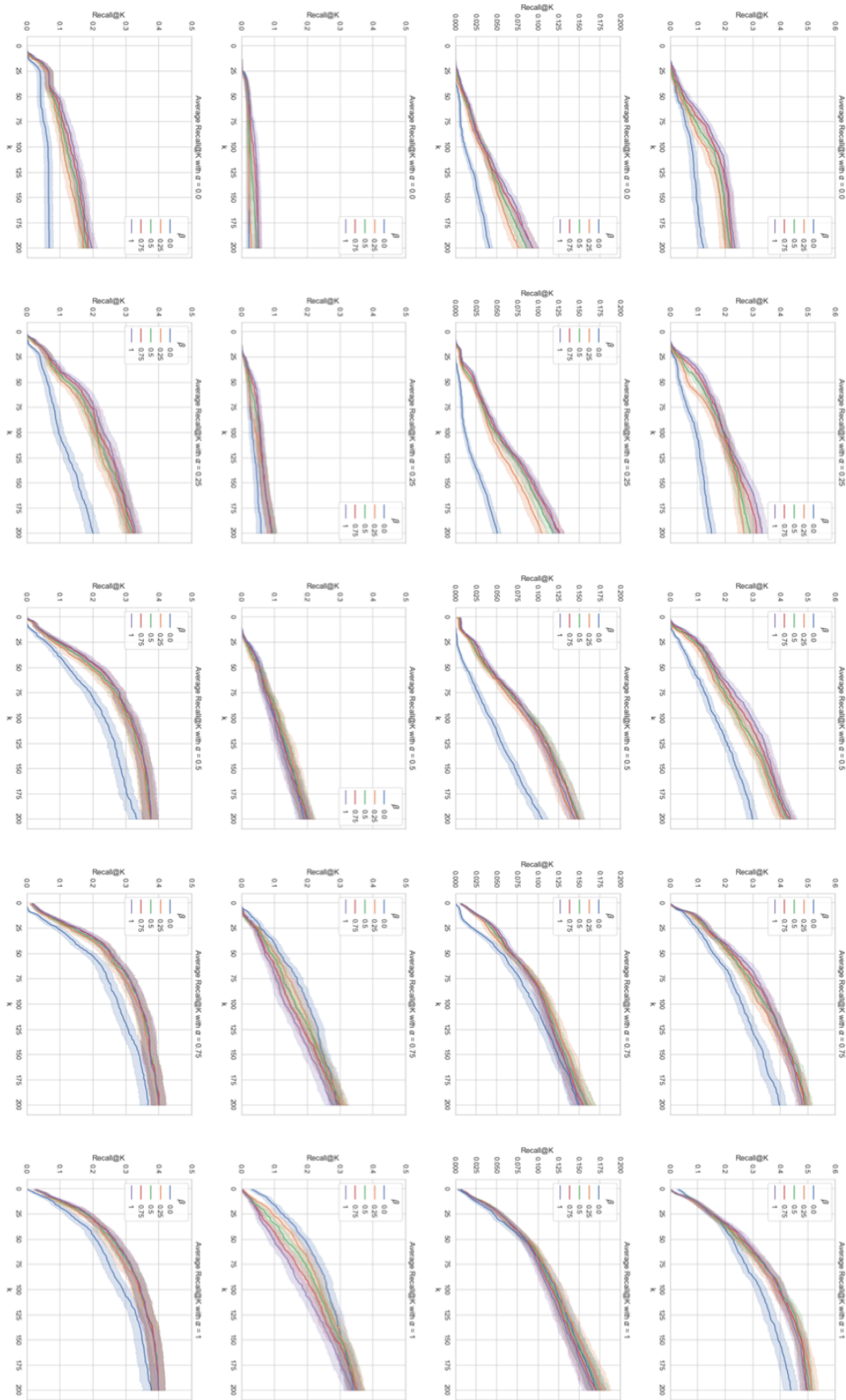


Supplementary Fig. 6: Benchmark on each cancer disease analyzed to pick the best combination of hyper parameters  $(\alpha, \beta, r)$ . Tab **a)** shows the comparison with respect to Recall@k and Tab **b)** comparison with respect to nDCG, for different values of the teleporting probability. Regardless of the choice of  $r$ , results (in terms of Recall@k and nDCG) were best when  $\alpha = 1$  and  $\beta = 0.5$ . These values correspond to i) considering only ontologies to the purpose of computing personalization vectors and ii) giving equal importance to ontologies and gene expression when computing the transition matrix of the random walk.

a bias on the ontologies (GO biological processes, KEGG and Reactome pathways). Indeed, the best performance are obtained for large values of  $\alpha$  as shown in Supplementary Fig. 7. I.e., it is better to teleport to biologically similar proteins than differentially expressed genes. As regards the aggregated transition matrix, performance in terms of Recall@k/nDCG is maximized when  $\beta = 0.5$ . In other words, performance is maximized when co-expression information is combined with biological information (and the PPI). Once we discovered the best combination of  $(\alpha, \beta)$ , we tried different values of the restart probability, with results summarized in Supplementary Fig. 6. As Supplementary Fig. 6 shows, results are not greatly affected by the value of the restart probability, as long this as this exceeds the value 0.25.

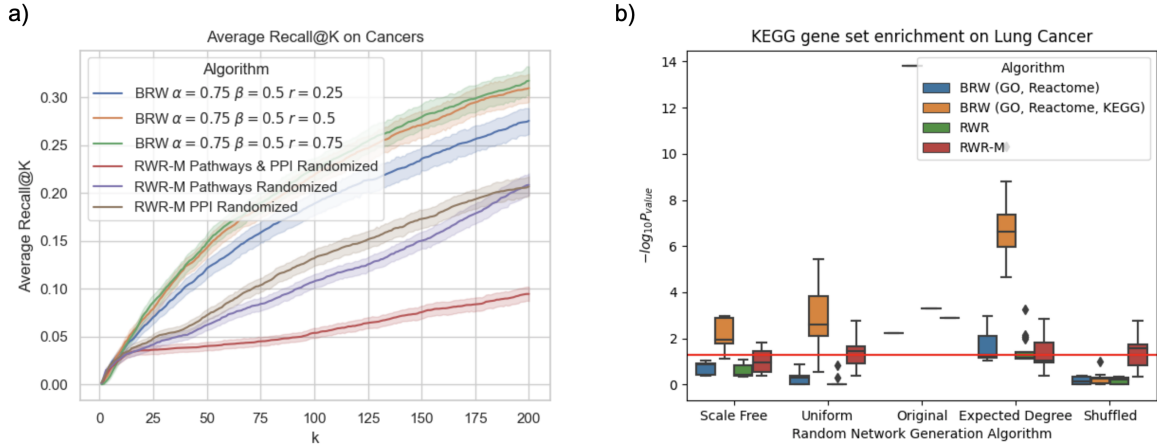
**Drug target discovery and drug enrichment.** In this case, we considered Breast Cancer phenotype and we analyzed drug enrichment and performance in drug target discovery of each combination of hyper-parameters  $(\alpha, \beta, r)$ , in terms of Recall@k and nDCG. Table 3 shows the result of the drug enrichment, Recall@k, nDCGs and number of FDA approved, Breast Cancer drugs that were annotated, for each combination of parameters. As shown in the table, different parameter combinations perform best for different validation tasks. For example, parameter combinations corresponding to a bias toward ontologies perform best in the task of identifying Breast Cancer drug targets of approved drugs, highly scoring drug targets in the first 200 positions, whereas biasing the random walk towards differentially expressed genes and the co-expression network performs best in prioritizing genes that are enriched in many relevant drugs. Indeed, Paclitaxel, Fulvestrant, Doxorubicin, Tamoxifen, Methotrex-





Supplementary Fig. 7: Benchmark on each cancer disease analyzed to identify the best combination of pair of hyper parameters  $(\alpha, \beta)$ . Each row represents the following tumor type analyzed in this manuscript: BRCA, LUAD, THCA, and COAD. Each row plots the comparison of different runs of the BRW for same value of  $\alpha$  and different values of  $\beta$ , while restart probability is set to 0.5 in all experiments.

### C.3 Robustness and Bias



Supplementary Fig. 8: BRW and RWR-M comparison. Tab a) shows the comparison between BRW and RWR-M on ranking test known disease genes when at least one network is randomized. As we can see, enriched ontologies (GO biological Processes, Pathways) correlate positively between seed and validation set. Consequently, the noise induced by the randomized PPI is mitigated. Unfortunately, even if RWR-M relies on several biological information (PPI- Network, CO-Expression Network and Pathways Network) it is not able to mitigate the noise as much is mitigated by Biological Random Walks. Tab b) illustrates how multi-omics integration affect the bias induced by curated ontologies (GO, Reactome) and the PPI network

In a first experiment, we performed a mean 100-fold validation for each cancer phenotype by randomly sampling 70% of known disease genes and using the rest to compute the average Recall@k of each tested algorithm. To begin, we tried different values of the restart probability to understand how the biologically weighted teleporting probability is correlated with the test genes. We found out that this correlation is strong, and thus when a very high restart probability is used, BRW improves its prediction performances, as shown in Supplementary Fig. 8 a).

In a second round of experiments, we tried to understand what biological information used by RWR-M was critical for test gene retrieval. To this purpose, we started by only randomizing only the PPI network and keeping the original pathways network used by RWR-M. In a second step, we did the opposite. We discovered that the bias induced by Graphite is more critical in predicting test genes than using the original PPI network. Indeed, Supplementary Fig. 8 a) shows that the average Recall of the first 200 positions computed on the randomized PPI network is always higher than the average Recall@k compute when we randomize the (pathways) Graphite network. Finally, we executed RWR-M using randomized versions of both networks as inputs to the algorithm, and its prediction performance dropped drastically.

Furthermore, to understand if candidate genes predicted using randomized PPI networks are more biologically meaningful than those returned using the original PPI, we considered the test suite proposed by [LBLB21]. We evaluated RWR-M and BRW on the Lung Cancer phenotypic condition using the BIOGRID PPI network, both implemented in the test suite. Since RWR based algorithms depend on restart probability (i.e., greater values of  $r$  make the algorithms depend less on the topology of the network and, in the extreme case when  $r = 1$ , the Markov chain converges to the personalization vector making the topology of the network completely useless), we set  $r = 0.25$ . Moreover, we chose  $\alpha = 1$  and  $\beta = 1$  when running BRW; in this way, we isolated the bias induced by manually curated ontologies and not by gene expression. We then validated each predicted gene set using gseapy KEGG Pathways enrichment analysis implemented in the test suite and we compared the outcomes returned using the original PPI with those obtained using its randomized counterparts: uniform, scale-free, expected degree, and shuffled.

Supplementary Fig. 8 b) shows the comparison between candidate genes predicted using a randomized

network and the original one. The x axis represents all randomized methods that are available in the test suite, while the y axis represents the negative log scale of p-values calculated by the test suite using KEGG enrichment analysis provided by **gseapy** on predefined Lung Cancer pathways.

## C.4 Comparison with [GMP+19]

BRW is the evolution of a framework we proposed in [GMP+19] in its embryonic form. Both rely on the hypothesis that genes involved in the same disease should be more likely to share biological similarities. [GMP+19] is different from the current work in significant ways. Our initial approach integrated only Gene Ontology to define the personalization vector and the transition matrix of the random walk, something that was done in an ad-hoc way. In contrast, the framework proposed in this paper proposes a principled approach, described in Section 2 of the main paper and Sections B.3.2 and B.4.4 of this supplementary material, whereby multiple, heterogeneous biological datasets such as KEGG, Reactome, and GO, can be seamlessly integrated to define a biased random walk with restart. In particular, this new version effectively integrates differential expression and co-expression data to improve the biological meaning of candidate genes prioritized in the top K positions. To demonstrate the power of incorporating multi-omics data (i.e., Proteome and Transcriptome) and several manually curated ontologies (i.e., KEGG, Reactome, and GO), in this section, we compare our framework with the algorithm proposed in [GMP+19]. In the paragraphs that follow, the latter is referred to as BRW CIBCB 2019.

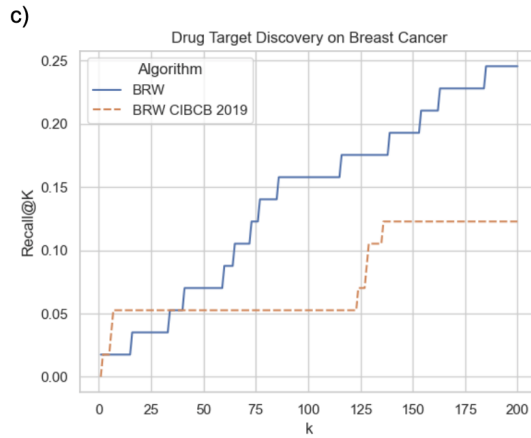
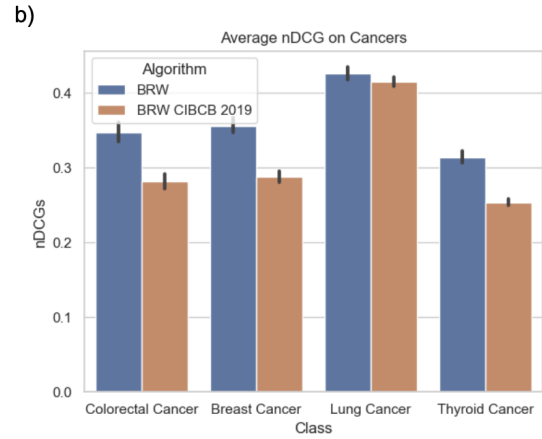
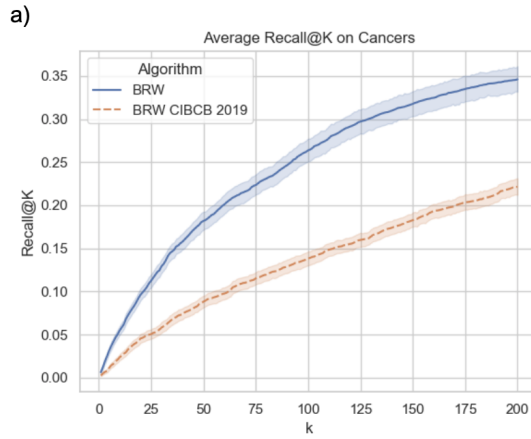
We compared our approach with [GMP+19] along two axes, similarly to what we did for other baselines: i) we performed a 100-fold Montecarlo random sample (internal) validation, dividing the set of known disease genes into a seed set and a test set, which we used to compute Recall@K and nDCG; ii) we further performed an external validation, to this purpose focusing on Breast Cancer and comparing the two competing approaches in terms of the set of statistically significant drugs they retrieve if we restrict to candidate genes ranked the first 200 positions.

Supplementary Figures 9 a) and b) compare our approach with BRW CIBCB 2019 in terms of average Recall@K and nDCG computed over the aforementioned 100-fold Montecarlo runs. BRW’s ability to leverage manually curated information from KEGG and Reactome and gene expression data (i.e., differential expression and co-expression network) drastically improves the algorithm’s performance in prioritizing known candidate genes from the test set.

In the case of drug targets, the fraction of drug targets discovered by BRW consistently increases with the number  $k$  of top ranked genes we consider, showing a two-fold improvement over [GMP+19] (Figure 9 c)). This behaviour is further confirmed if one considers Breast Cancer drugs that are enriched by genes in top 200 positions. In particular, Figure 9 d) shows that BRW returns a list of candidates enriched in doxorubicin, methotrexate and tamoxifen, all well-known drugs to treat Breast Cancer (<https://www.cancer.gov/about-cancer/treatment/drugs/breast>).

Table 4: Drugs approved to treat Breast Cancer which have at least one drug target predicted by at least one framework. If an algorithm prioritize a target of a specific drug, its cell is highlighted and it contains 1. The combination of Hyper-parameters used by BRW is  $\alpha = 0.75$ ,  $\beta = 0.75$ ,  $r = 0.25$

| Drug Bank ID | Drug Name            | Associated Condition                  | BRW | DADA | DIAMOnD | RWR-M | RWR |
|--------------|----------------------|---------------------------------------|-----|------|---------|-------|-----|
| DB12001      | Abemaciclib          | Metastatic HR + HER2 - breast cancer  | 1   | 0    | 0       | 0     | 0   |
| DB00675      | Tamoxifen            | Breast Cancer                         | 1   | 1    | 1       | 1     | 1   |
| DB11828      | Neratinib            | Breast Cancer                         | 1   | 1    | 0       | 1     | 1   |
| DB01259      | Lapatinib            | Metastatic Breast Cancer              | 1   | 1    | 0       | 1     | 1   |
| DB09073      | Palbociclib          | Metastatic Breast Cancer              | 1   | 0    | 0       | 0     | 0   |
| DB11730      | Ribociclib           | Metastatic Breast Cancer              | 1   | 0    | 0       | 0     | 0   |
| DB00072      | Trastuzumab          | Breast Cancer                         | 1   | 1    | 0       | 1     | 1   |
| DB00570      | Vinblastine          | Refractory Breast cancer              | 1   | 1    | 1       | 1     | 0   |
| DB11760      | Talazoparib          | Metastatic Breast Cancer              | 1   | 0    | 1       | 0     | 0   |
| DB09074      | Olaparib             | Metastatic Breast Cancer              | 1   | 0    | 1       | 0     | 0   |
| DB00624      | Testosterone         | Inoperable, metastatic Breast cancer  | 1   | 1    | 1       | 1     | 1   |
| DB06710      | Methyltestosterone   | Metastatic Breast Cancer              | 1   | 1    | 1       | 1     | 1   |
| DB01248      | Docetaxel            | Metastatic Breast Cancer              | 1   | 1    | 0       | 0     | 1   |
| DB01248      | Docetaxel            | Locally Advanced Breast Cancer (LABC) | 1   | 1    | 0       | 0     | 1   |
| DB08871      | Eribulin             | Refractory, metastatic Breast cancer  | 1   | 1    | 0       | 0     | 1   |
| DB00286      | Conjugated estrogens | Metastatic Breast Cancer              | 1   | 1    | 1       | 0     | 1   |
| DB00481      | Raloxifene           | Invasive Breast Cancer                | 1   | 1    | 1       | 0     | 1   |
| DB00445      | Epirubicin           | Breast Cancer                         | 0   | 0    | 1       | 0     | 0   |
| DB01204      | Mitoxantrone         | Metastatic Breast Cancer              | 0   | 0    | 1       | 0     | 0   |
| DB00997      | Doxorubicin          | Metastatic Breast Cancer              | 0   | 0    | 1       | 0     | 0   |



d)

| Enriched Drugs   | BRW CIBCB 2019 | BRW  |
|------------------|----------------|------|
| arsenic trioxide | 13.4           | 17.1 |
| dexamethasone    | 6.3            | 4.5  |
| metoprolol       | 6.1            | 3.3  |
| hydrocortisone   | 5.6            | 7.3  |
| doxorubicin      | 4.7            | 7.6  |
| imatinib         | 4.4            | 10.3 |
| sirolimus        | 3.8            | 19.1 |
| cetuximab        | 2.9            | 5.6  |
| valproic acid    | 2.6            | 5.9  |
| hydroquinone     | 2.6            | 5.6  |
| vorinostat       | 2.3            | 9.1  |
| deferoxamine     | 2.2            | 5.4  |
| estradiol        | 2.1            | 11.6 |
| vitamin c        | 2              | 8.8  |
| methotrexate     | 1.9            | 6.3  |
| cisplatin        | 1.7            | 6    |
| trovafloxacin    | 1.5            | 6.2  |
| bexarotene       | 1.5            | 11   |
| mifepristone     | 1.3            | 6.9  |
| vincristine      | 1.1            | 6.3  |
| etoposide        | 1              | 6.4  |
| tamoxifen        | 0.9            | 6.4  |
| zinc acetate     | 0.8            | 6.1  |

Supplementary Fig. 9: Old vs New Approach comparison: a) and b) compare respectively the Recall@K and nDCG of the previous version of BRW with the one presented in this manuscript. c) compares BRW CIBCB 2019 with BRW on the percentage of drug target prioritized in the top 200 positions. Finally, d) compares the drug enrichment computed using the first 200 candidate genes prioritized by the frameworks.